How can ice science satisfy the public attention in a warmer world?

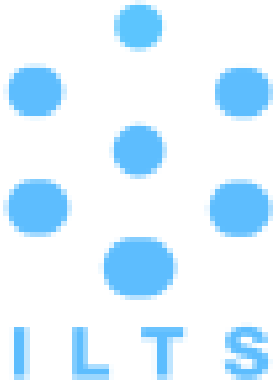

AWI ice science

(re-presented by Frank Wilhelms)

ILTS International Symposium
„Frontier of Low Temperature Science“
Sapporo, 9-10. November 2009

HELMHOLTZ ASSOCIATION

When will the Northern Sea Route be open?

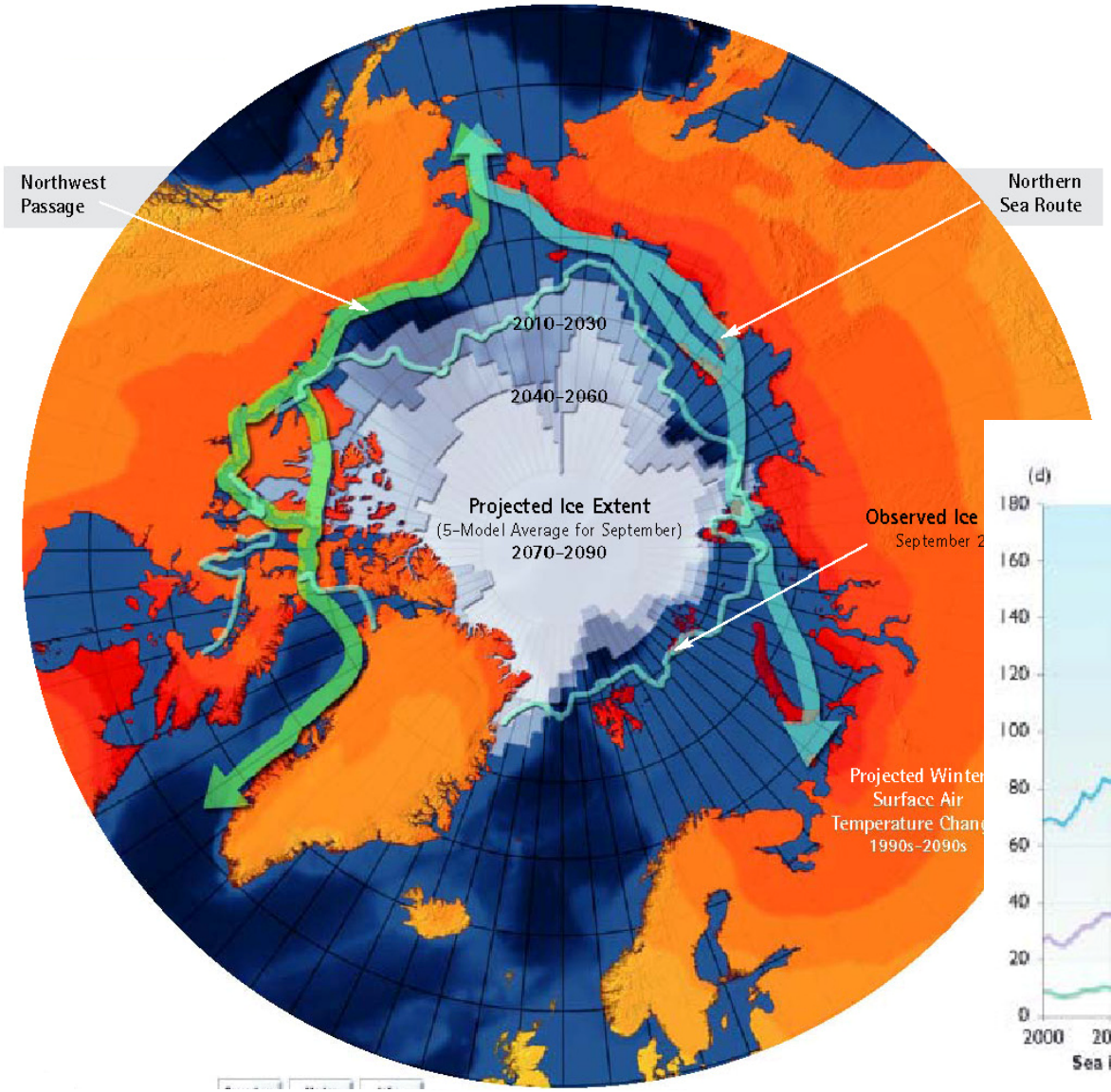

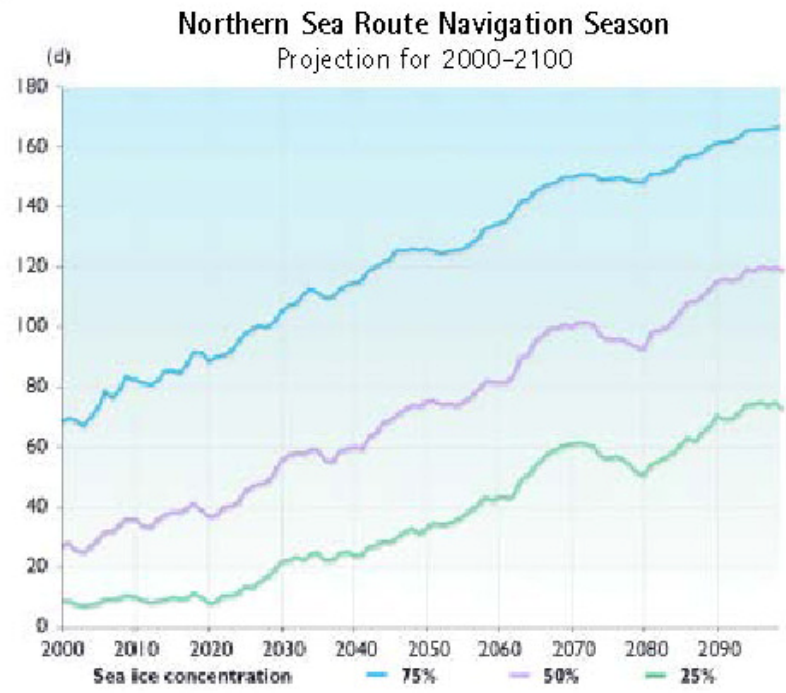

Arctic Climate Impact Assessment, Cambridge University Press, 2004

Journal of Applied Geophysics 67 (2009) 234–241

Contents lists available at ScienceDirect

Journal of Applied Geophysics

journal homepage: www.elsevier.com/locate/jappgeo

Helicopter-borne measurements of sea ice thickness, using a small and lightweight, digital EM system

Christian Haas [a,1,*], John Lobach [b], Stefan Hendricks [a], Lasse Rabenstein [a], Andreas Pfaffling [a,2]

[a] *Alfred Wegener Institute for Polar and Marine Research, Bussestrasse 24, D-27570 Bremerhaven, Germany*
[b] *Ferra Dynamics Inc., 4070 Powderhorn Cres., Mississauga, Ontario, Canada L5L 3B9*

Fig. 2. AWI EM bird during take-off from the helicopter deck of an icebreaker, North Pole 2001.

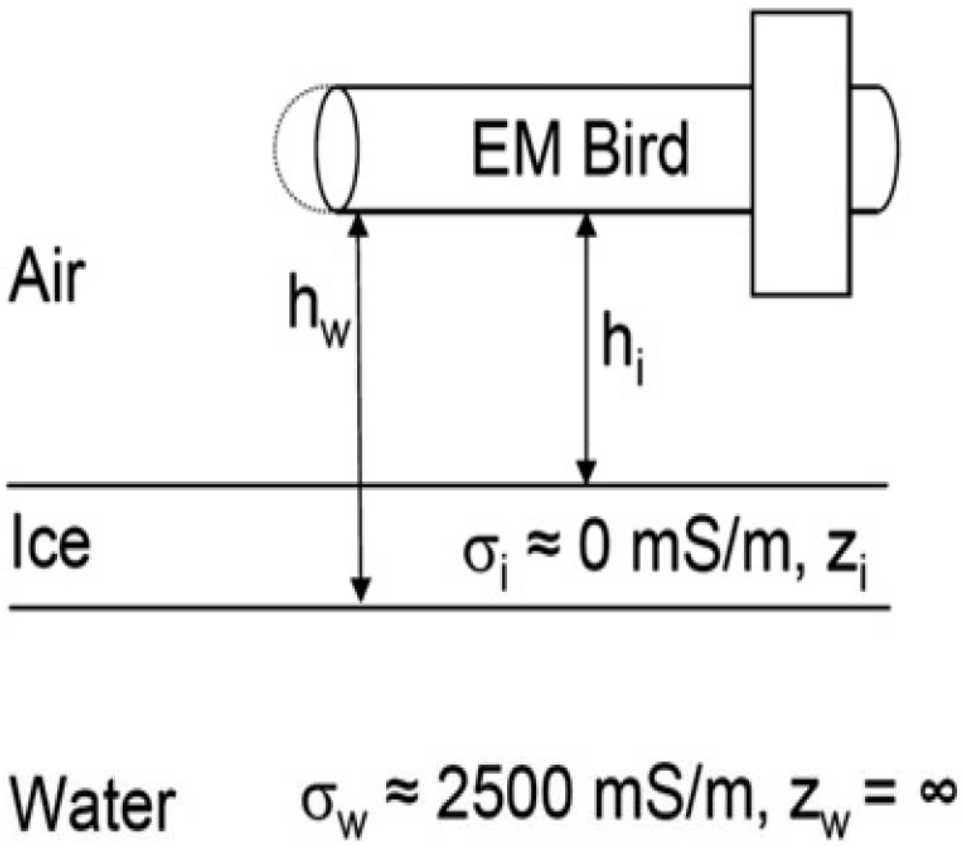

Fig. 1. Principle of EM thickness sounding, using a bird with transmitter and receiver coils and a laser altimeter. Ice thickness Z_i is obtained from the difference of measurements of the bird's height above the water and ice surface, h_w and h_i, respectively. h_w is obtained with the assumption of a negligible ice conductivity σ_i, known water conductivity σ_w, and horizontal layering.

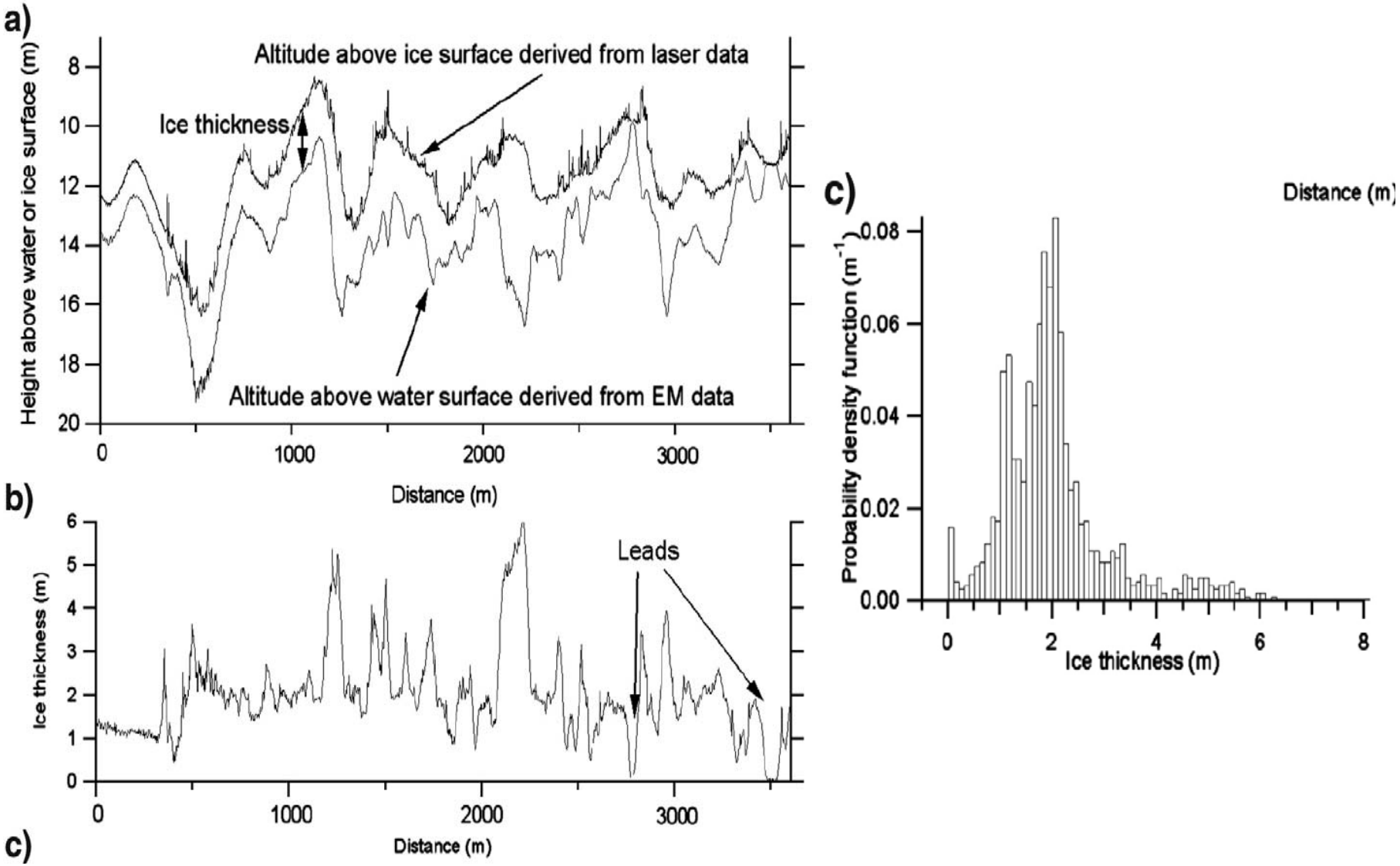

Fig. 8. (a) EM and laser derived bird height above the water h_w and ice surface h_i, respectively, and (b) ice thickness profile resulting from subtraction of the latter from the former. (c) Resulting thickness distribution.

EM Bird on Polar 5

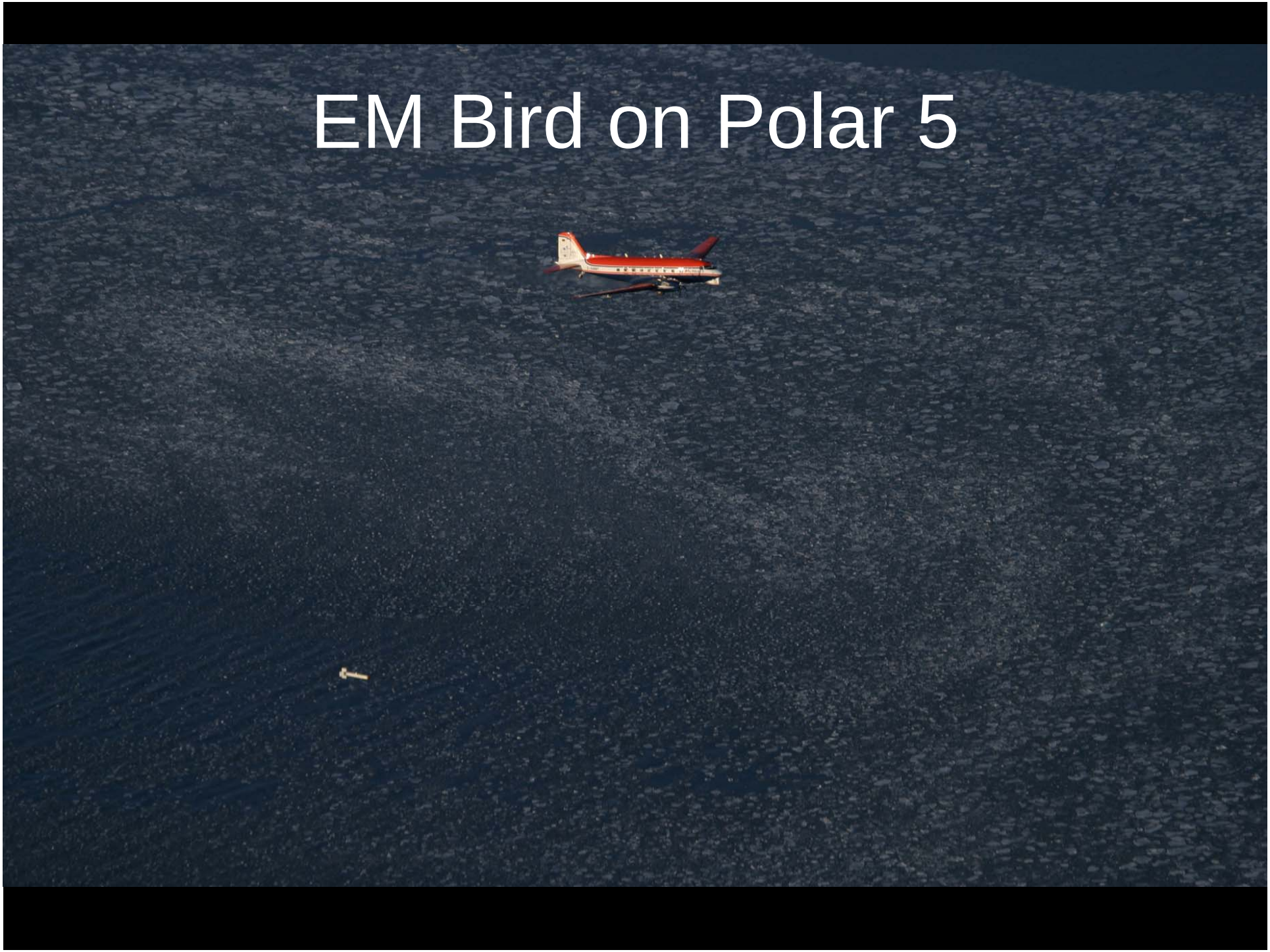

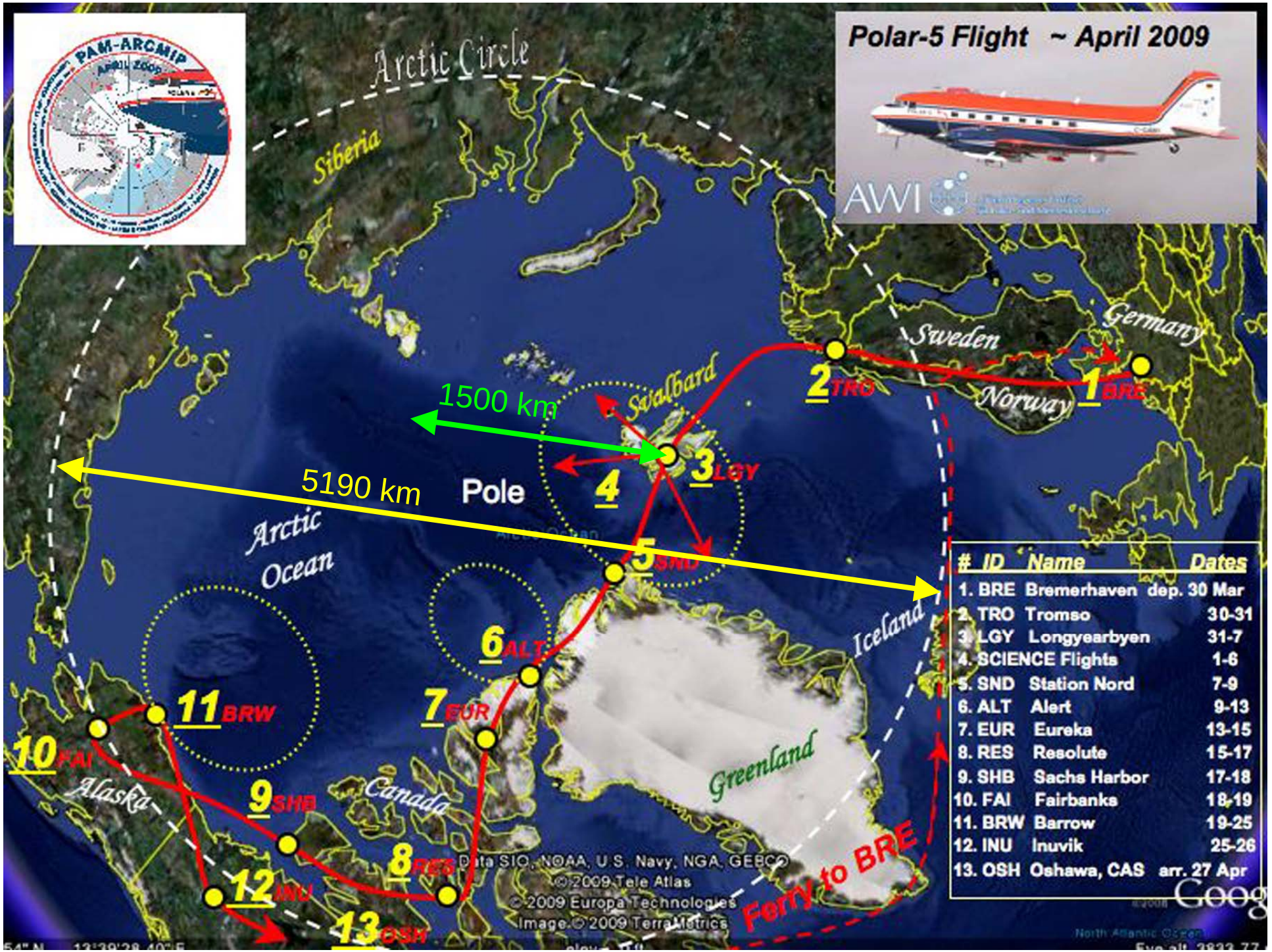
PAM-ARCMIP
Polar-5 Flight ~ April 2009
AWI
Arctic Circle
Siberia
Sweden
Germany
Norway
Svalbard
1500 km
5190 km
Pole
Arctic Ocean
Iceland
Greenland
Alaska
Canada
2 TRO
1 BRE
3 LGY
4
5 SND
6 ALT
7 EUR
8 RES
9 SHB
10 FAI
11 BRW
12 INU
13 OSH
Ferry to BRE
ID Name Dates
1. BRE Bremerhaven dep. 30 Mar
2. TRO Tromso 30-31
3. LGY Longyearbyen 31-7
4. SCIENCE Flights 1-6
5. SND Station Nord 7-9
6. ALT Alert 9-13
7. EUR Eureka 13-15
8. RES Resolute 15-17
9. SHB Sachs Harbor 17-18
10. FAI Fairbanks 18-19
11. BRW Barrow 19-25
12. INU Inuvik 25-26
13. OSH Oshawa, CAS arr. 27 Apr
Data SIO, NOAA, U.S. Navy, NGA, GEBCO
© 2009 Tele Atlas
© 2009 Europa Technologies
Image © 2009 TerraMetrics

How much will sea level rise at our shores in 100 years?

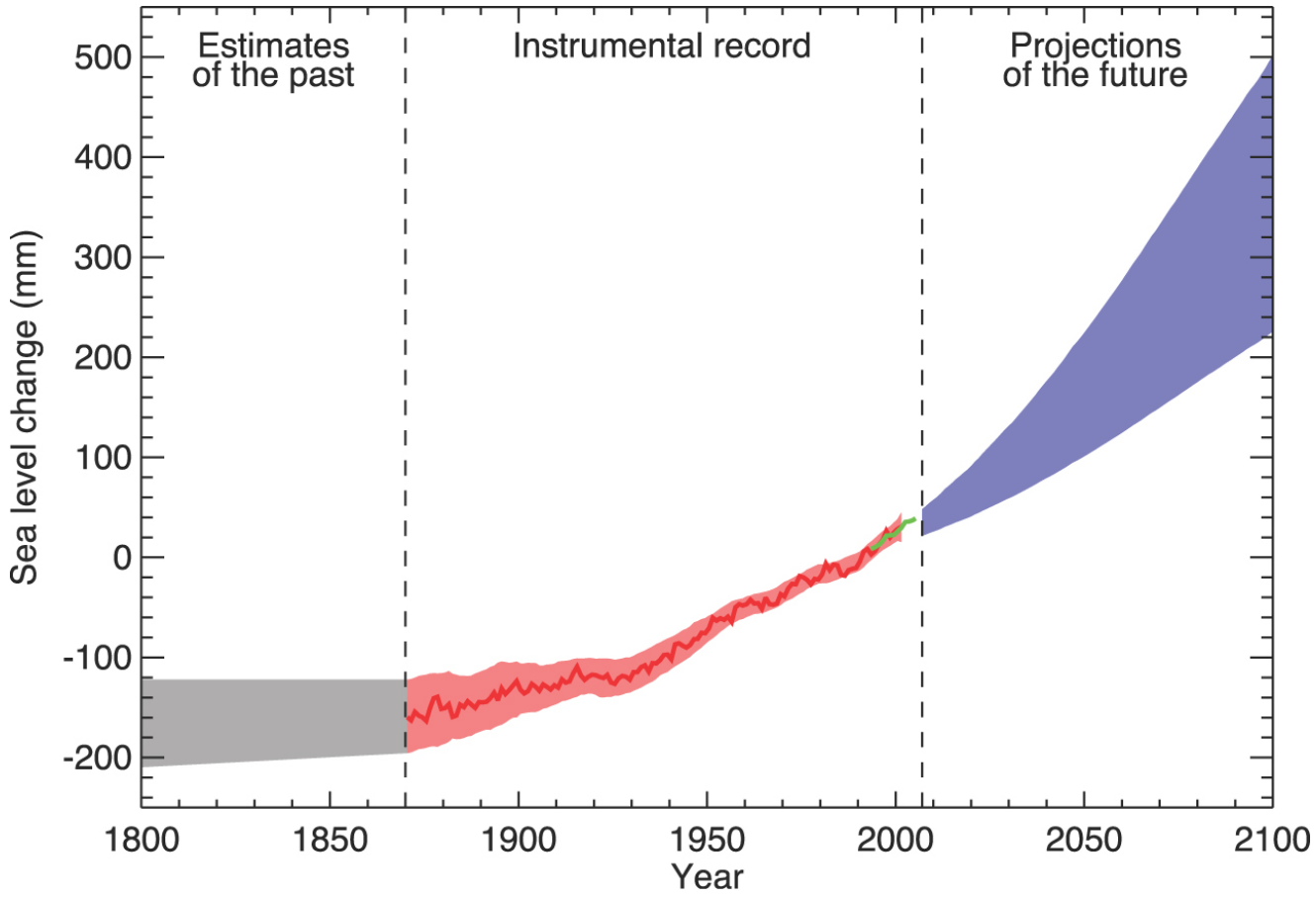

IPPC, 4th AR, chap. 5, Cambridge University Press, 2007

Sea level from observations

Short term trend of sea level

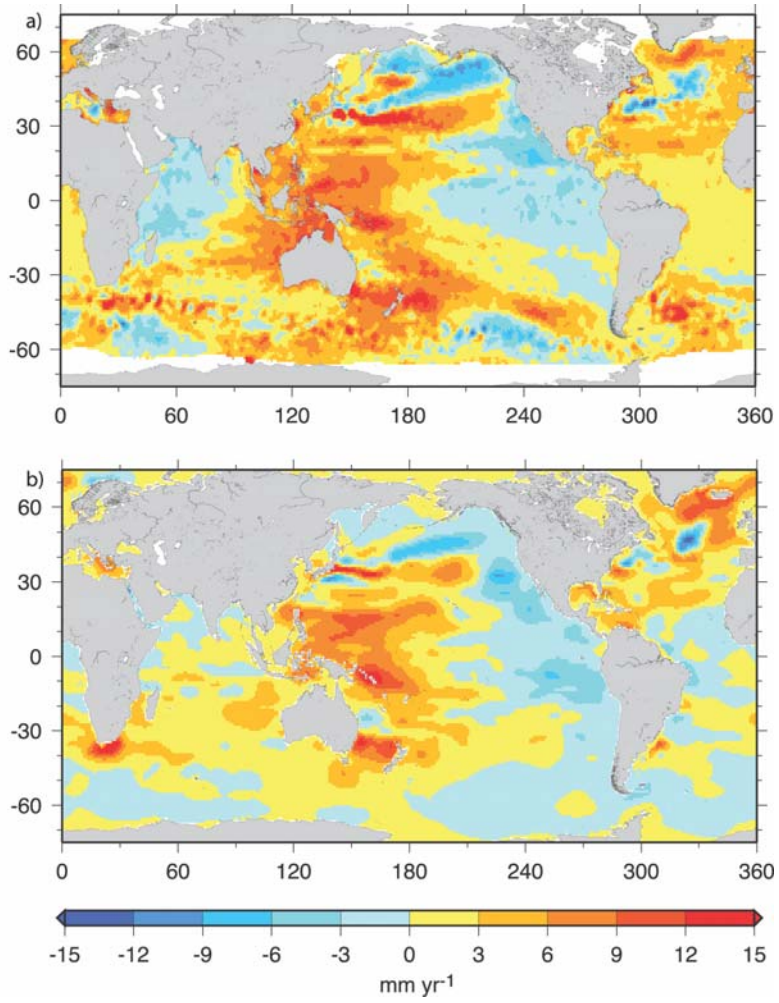

Short term trend of thermal expansion

Long term trend of sea level

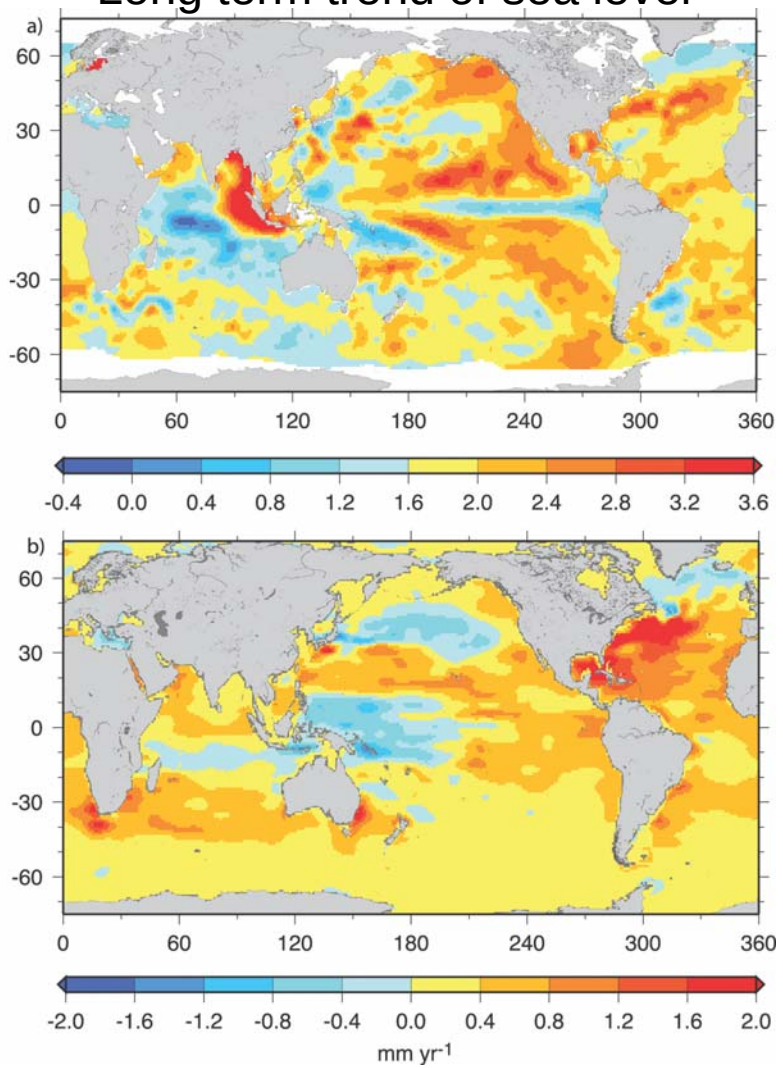

Long term trend of thermal expansion

IPPC, 4th AR, chap. 5, Cambridge University Press, 2007

The Cryosphere

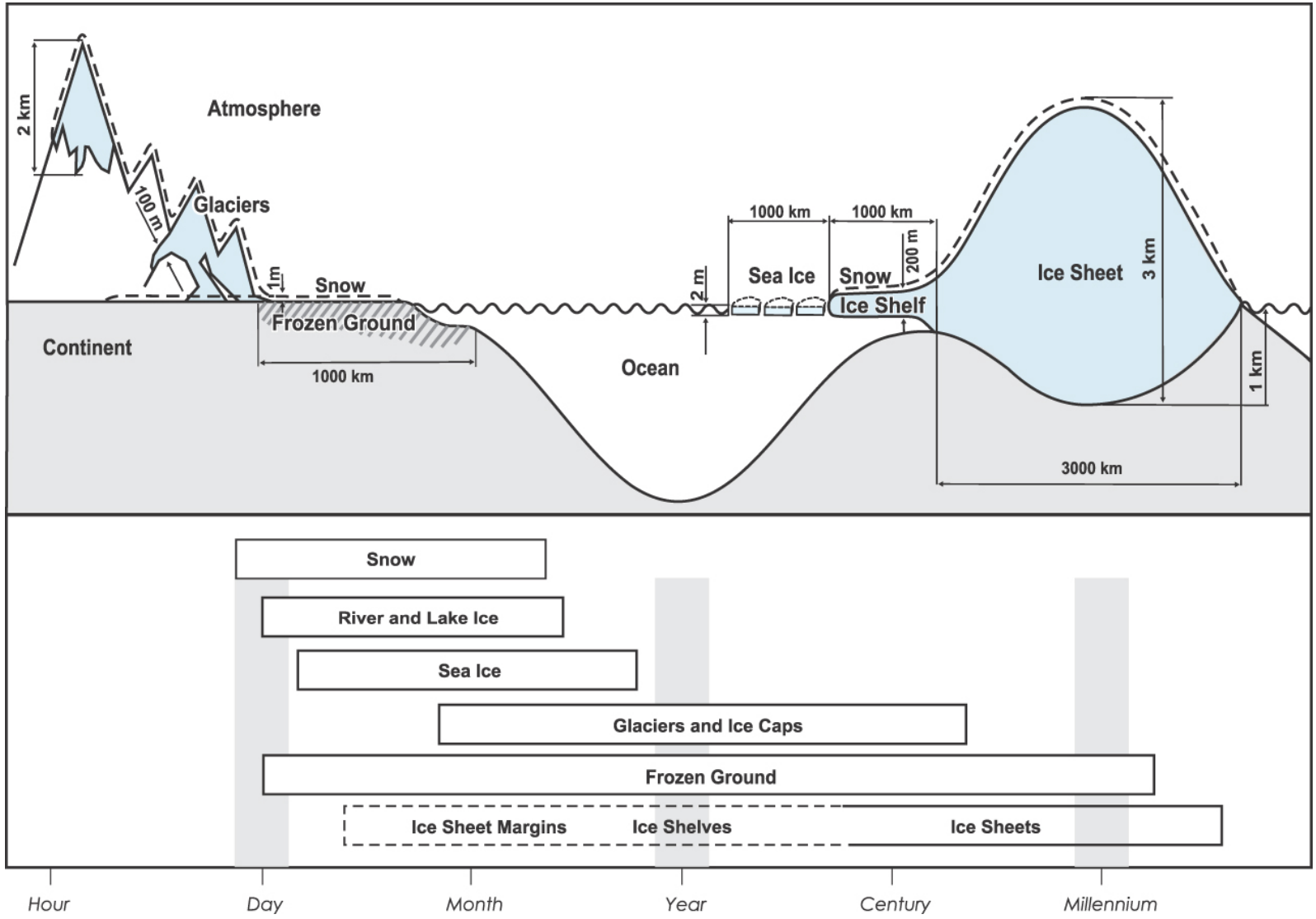

IPPC, 4th AR, chap. 4, Cambridge University Press, 2007

Contributions to sea level

Sea Level Rise (mm yr^{-1})			
Source	**1961–2003**	**1993–2003**	**Reference**
Thermal Expansion	0.42 ± 0.12	1.6 ± 0.5	Section 5.5.3
Glaciers and Ice Caps	0.50 ± 0.18	0.77 ± 0.22	Section 4.5
Greenland Ice Sheet	0.05 ± 0.12	0.21 ± 0.07	Section 4.6.2
Antarctic Ice Sheet	0.14 ± 0.41	0.21 ± 0.35	Section 4.6.2
Sum	1.1 ± 0.5	2.8 ± 0.7	
Observed	1.8 ± 0.5		Section 5.5.2.1
		3.1 ± 0.7	Section 5.5.2.2
Difference (Observed –Sum)	0.7 ± 0.7	0.3 ± 1.0	

IPPC, 4th AR, chap. 5, Cambridge University Press, 2007

Schematic Cross Section Through an Ice Sheet

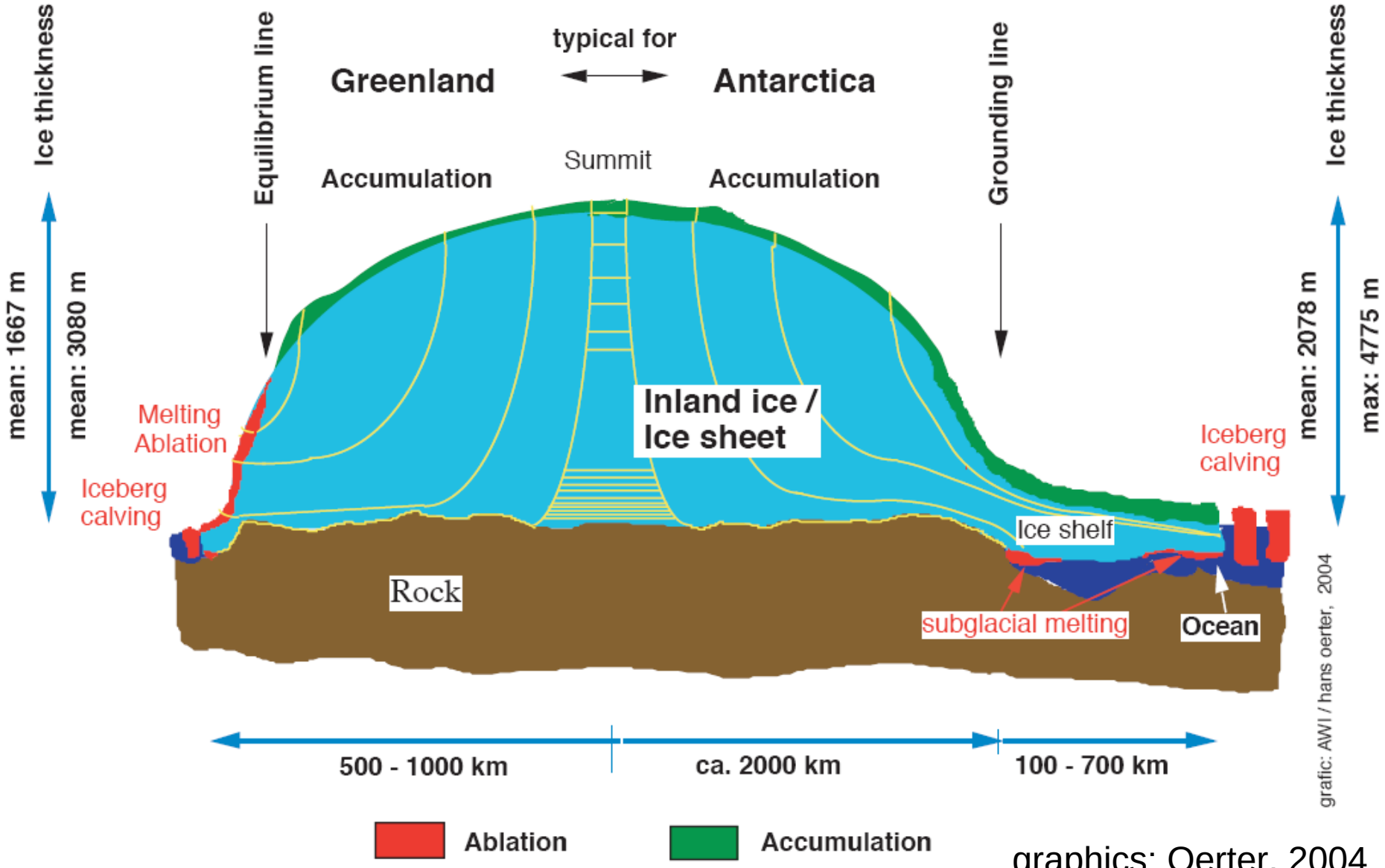

graphics: Oerter, 2004

Earth System Model at the AWI

Modules (following COSMOS)

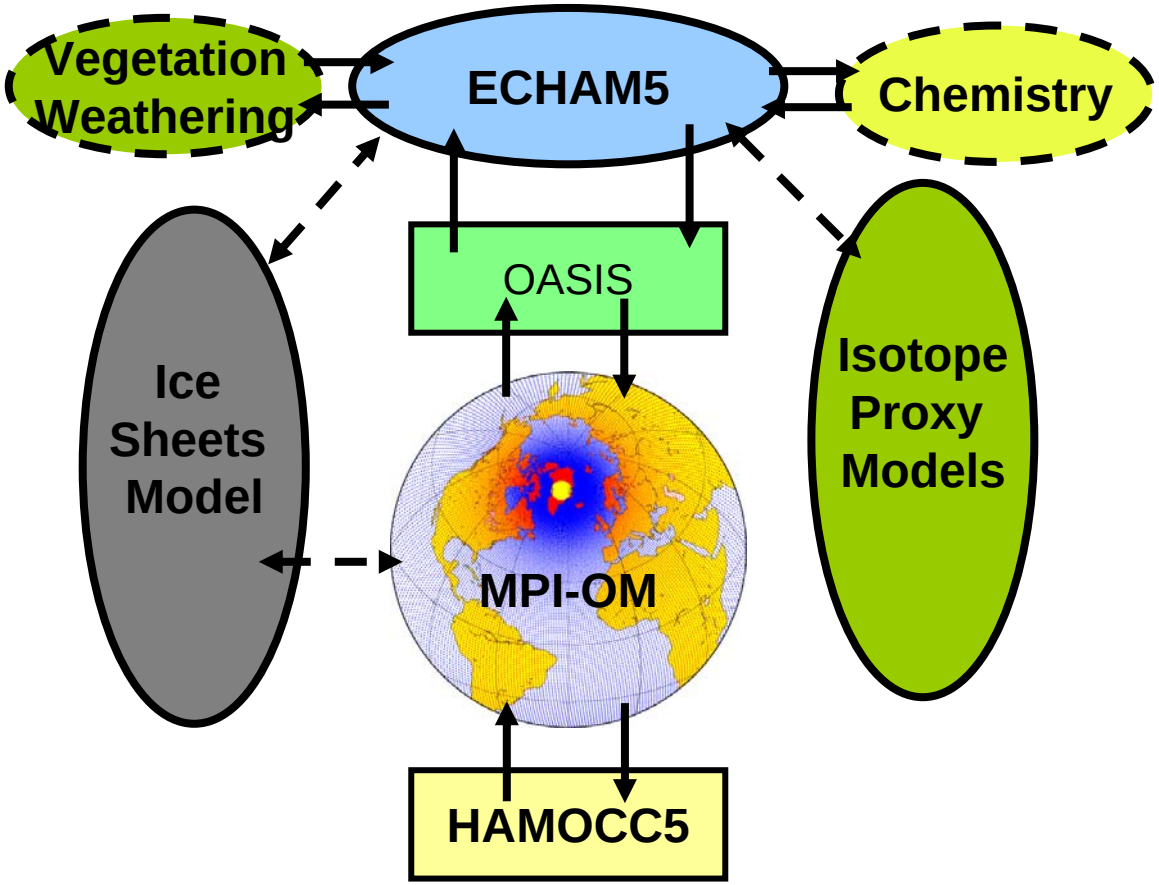

New modules:

Ice sheets model:
Mass balance & sea level
Ice-ocean interaction
Permafrost

Isotope modules:
Ice cores, Forams, Stalagmites

Biogeochemistry/Ecosystem
(based on Recom)
- marine biogeochemical cycles
- continental weathering input
- sediment module

Isotope transport in the Earth System

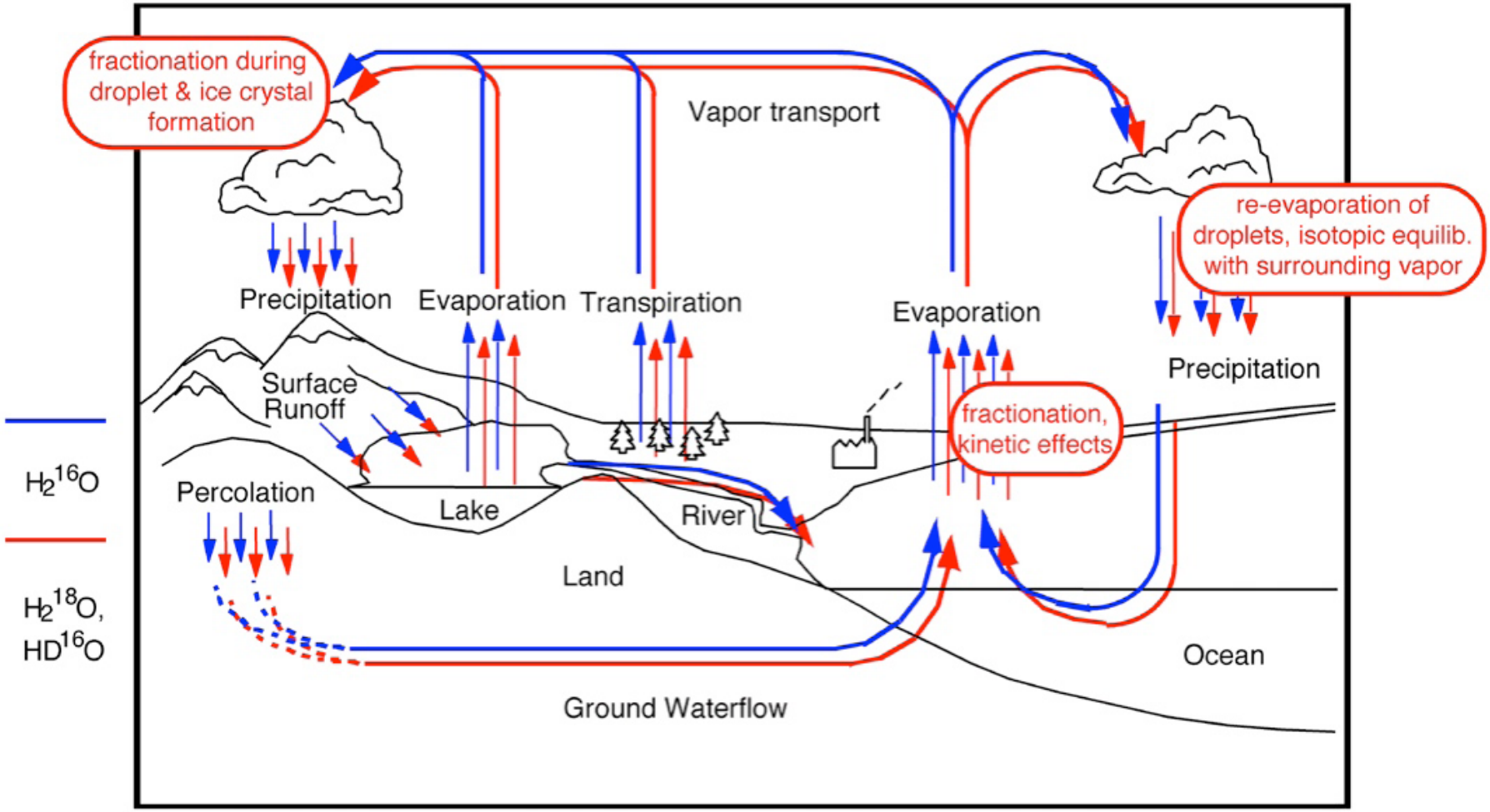

The ^{18}O Signal in Precipitation: Observations vs. Simulation

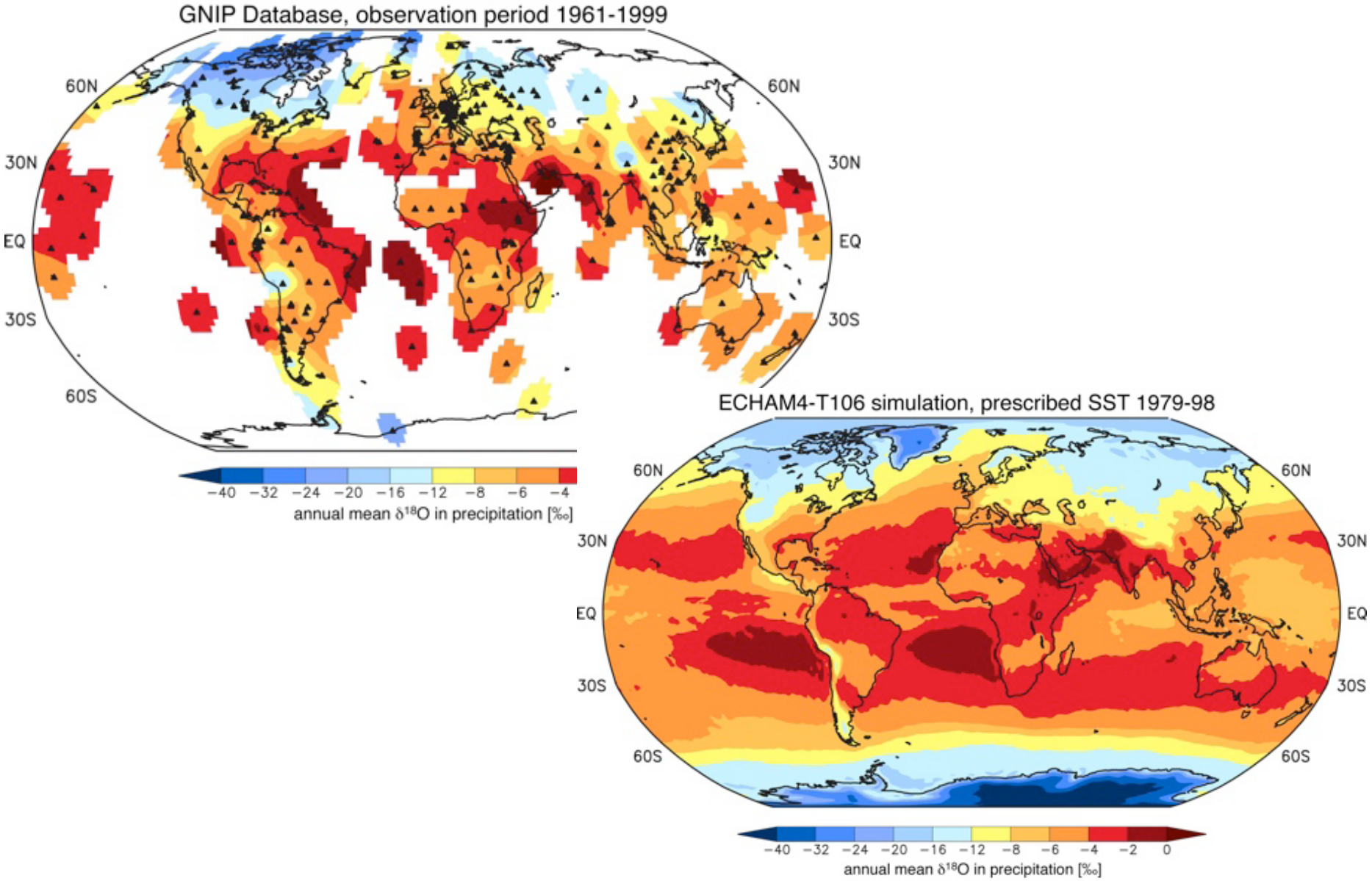

Ice-sheet model SICOPOLIS

Ice-sheet model SICOPOLIS (SImulation COde for POLythermal Ice Sheets):

3-d dynamic and thermodynamic ice-sheet model.

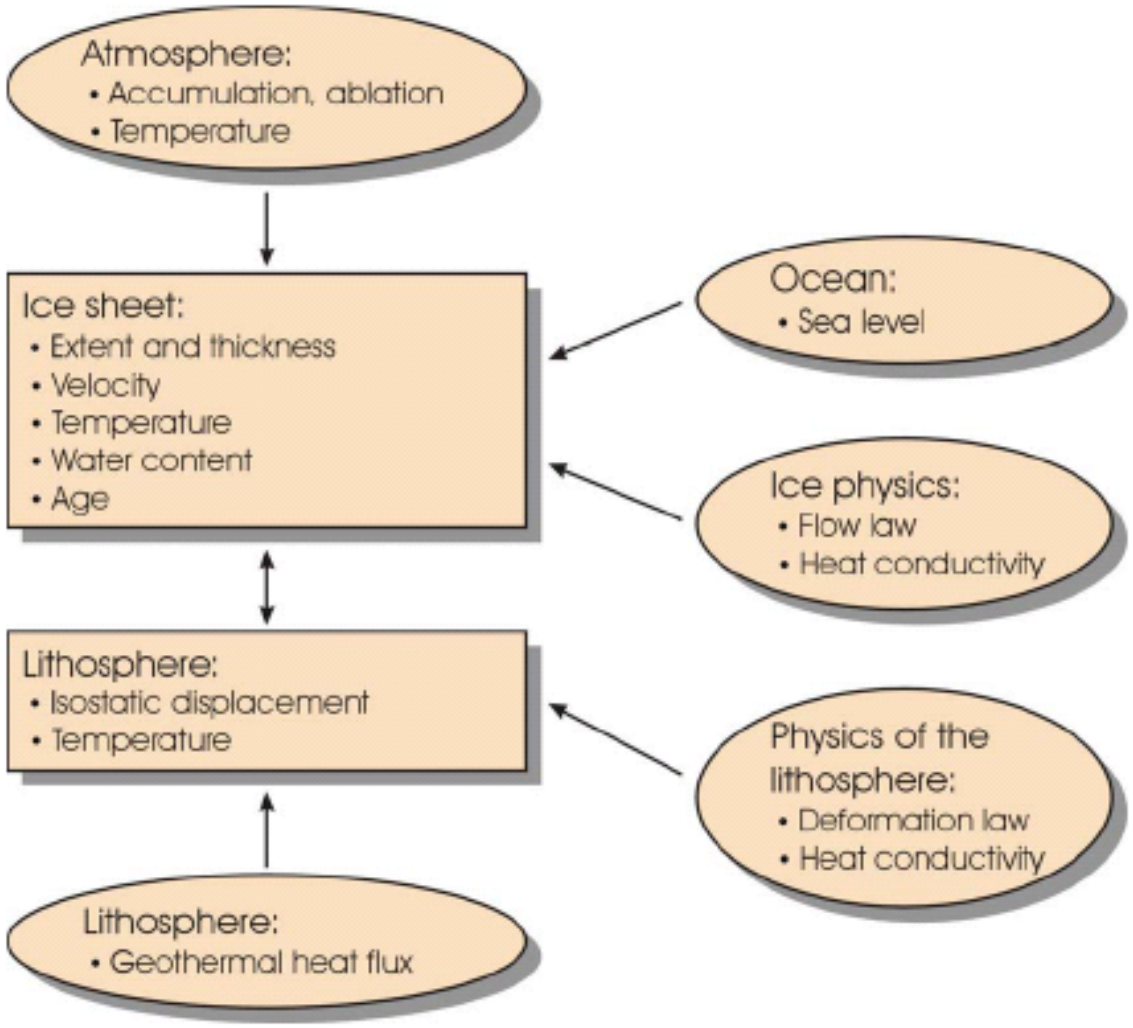

Tracer Trajectory simulation on Greenland Ice Sheet

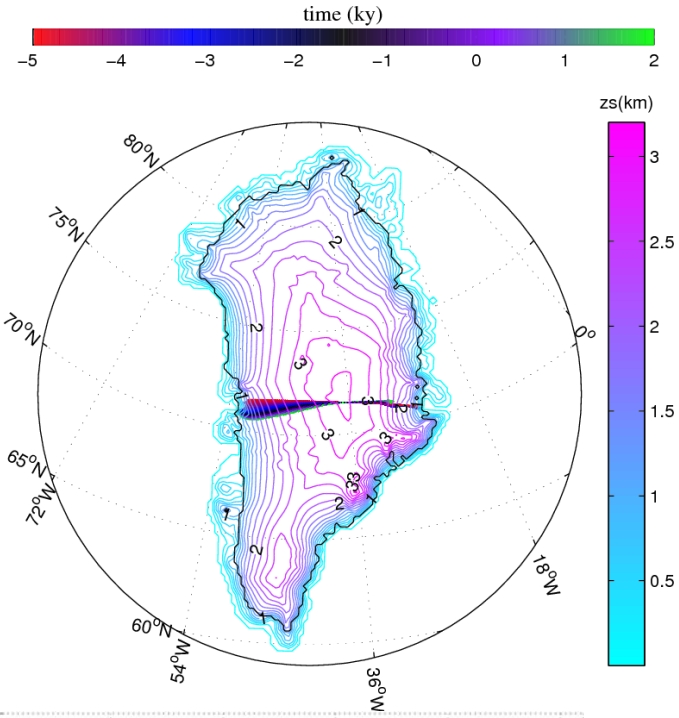

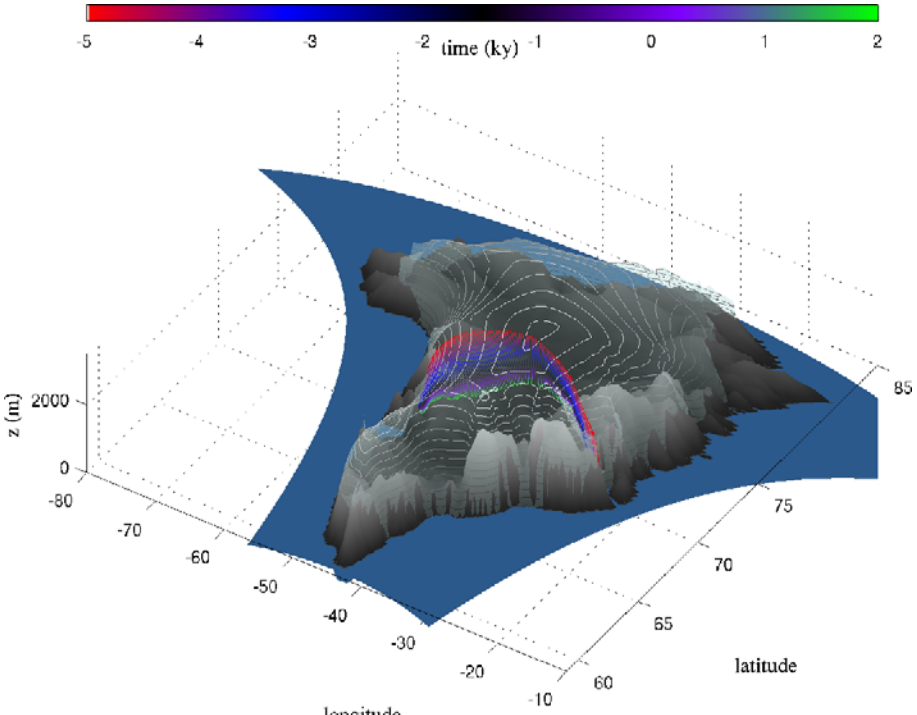

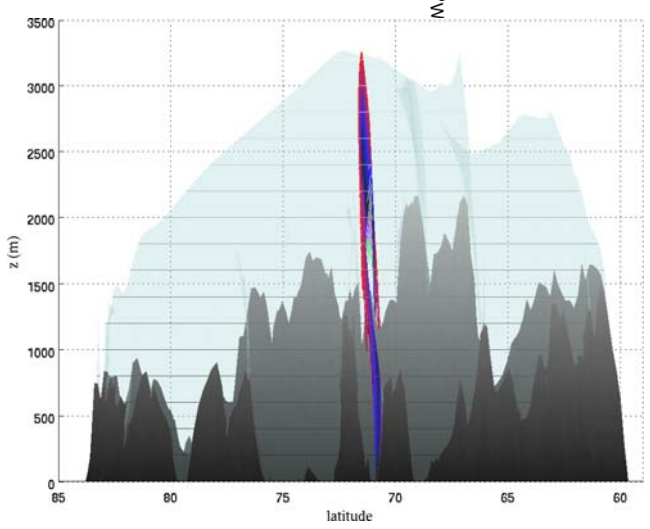

zonal view

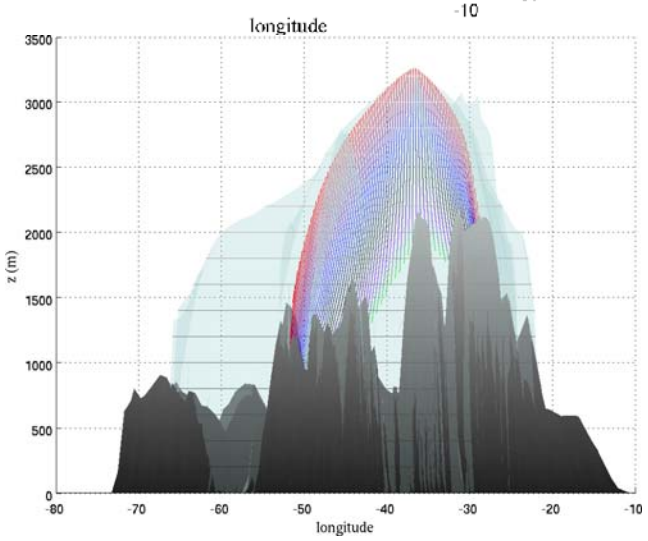

meridional view

Mapping of ice thickness and internal structure of ice sheets with the electromagnetic reflection method

POLAR 2 (D-CAWI)

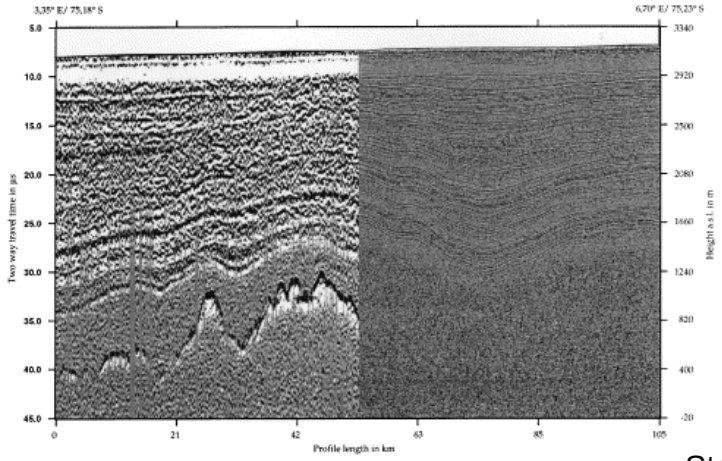

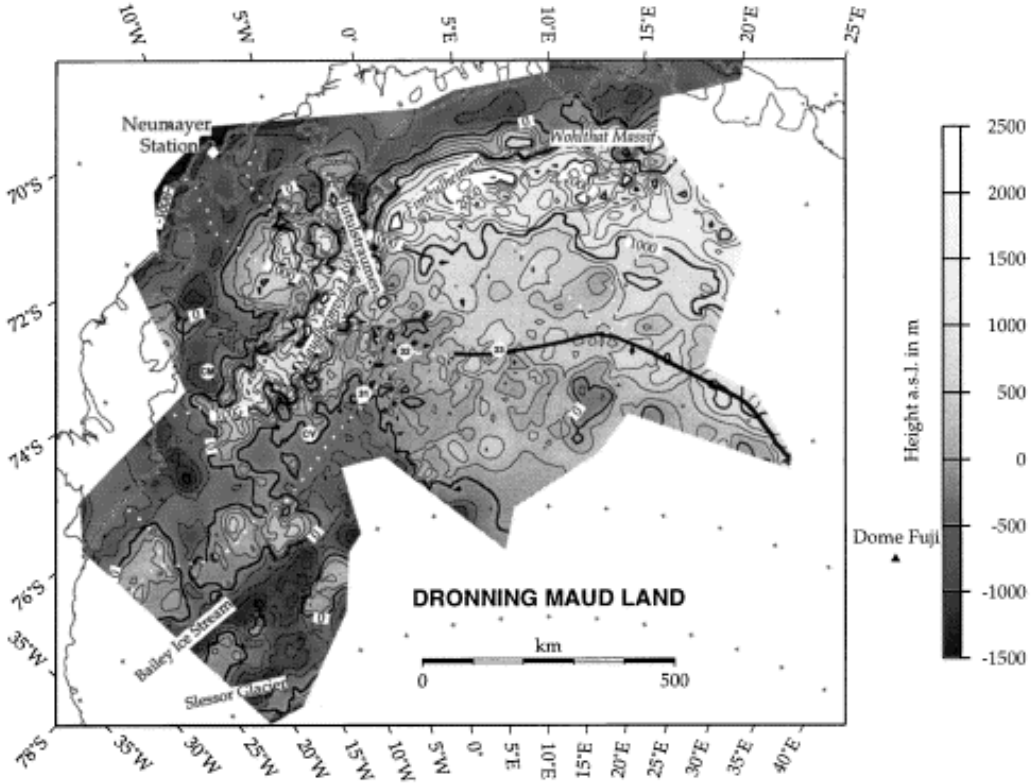

Steinhage *et.al., Journal of Applied Geophysics* 47 (3-4), pp. 183-189, 2001

volcanic horizons

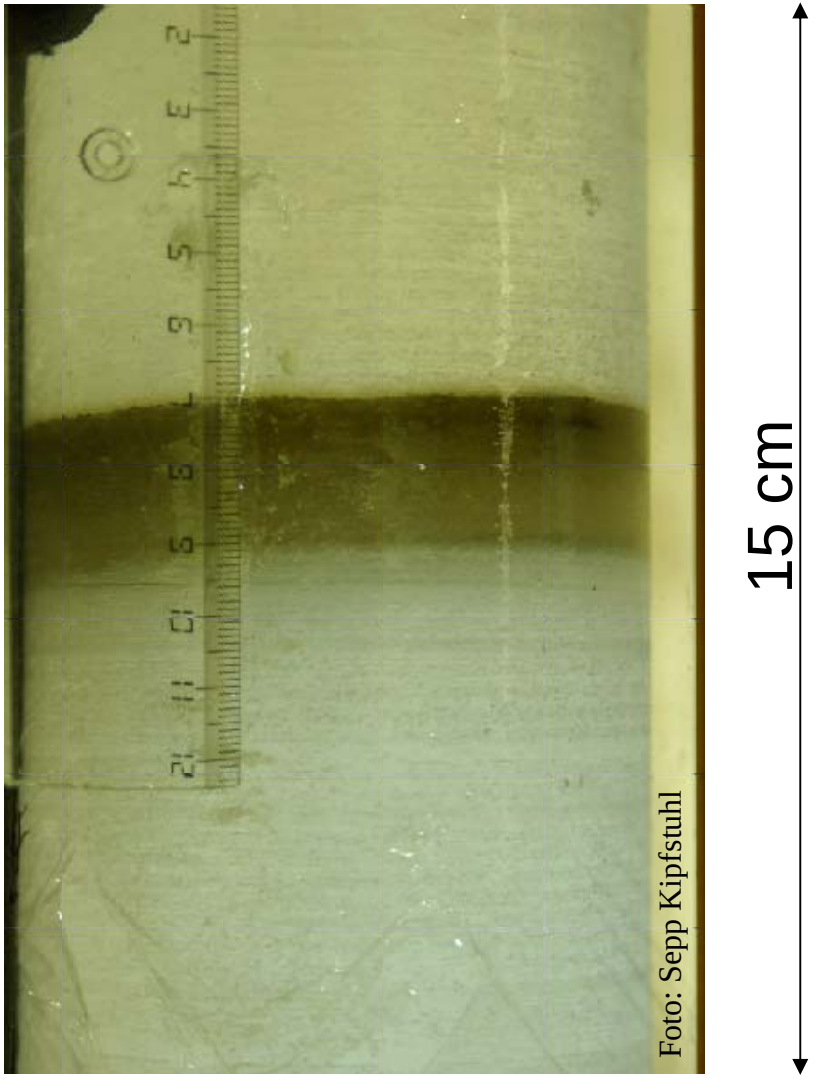

in 810 m depth (EDML)
(approx. 20 000 years old)

Internal structure of ice sheets

JOURNAL OF GEOPHYSICAL RESEARCH, VOL. 104, NO. B6, PAGES 13,013–13,024, JUNE 10, 1999

Nature of radio echo layering in the Antarctic ice sheet detected by a two-frequency experiment

Shuji Fujita,[1] Hideo Maeno,[2] Seiho Uratsuka,[2] Teruo Furukawa,[3] Shinji Mae,[1] Yoshiyuki Fujii,[3] and Okitsugu Watanabe[3]

Abstract. A two-frequency radio echo sounding experiment was carried out at Dome Fuji, the second highest dome in East Antarctica, and along a 1150-km-long traverse line from the dome to the coast. The goal was to determine the dominant causes of the radio echo internal reflections and to investigate their possible changes with depth ranges and regions. From the two-frequency (60 MHz and 179 MHz) radio echo responses at various sites, we distinguished four zones. Each of the zones is characterized by a dominant cause of radio echo internal reflection as follows. In the "P_D" zone, changes in dielectric permittivity are mainly due to density fluctuations; in the "P_{COF}" zone, changes in dielectric permittivity are mainly due to changes in crystal-orientation fabrics; and in the "C_A" zone, changes in electrical conductivity are mainly due to changes in acidity induced by past volcanic eruptions. In each of these three zones, the changes occur commonly along isochrones. In addition, a basal echo-free zone, the fourth zone, was found to appear always below the P_{COF} zone. These four zones and their distribution suggested variations of the physical conditions within the ice sheet.

[1] Department of Applied Physics, Faculty of Engineering, Hokkaido University, Sapporo, Japan

[2] Communications Research Laboratory , Ministry of Post, Tokyo.

[3] National Institute of Polar Research, Tokyo.

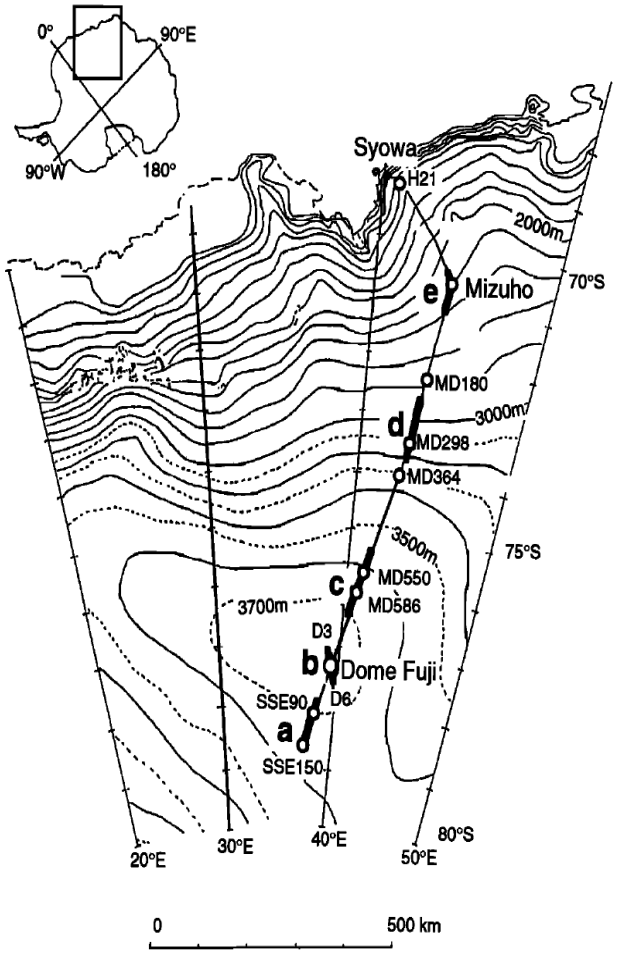

Figure 1. Elevation map of East Antarctica, showing the location of the 1150-km-long traverse route from the site "SSE150" through Dome Fuji to the coast. Circles indicate sites of detailed local measurements. The five bold lines (indicated by a-e) are sections of the traverse line used in cross-section analyses in Figures 2 and 3, and Plate 2. Note that line b is at an angle to the profile line of Figure 2.

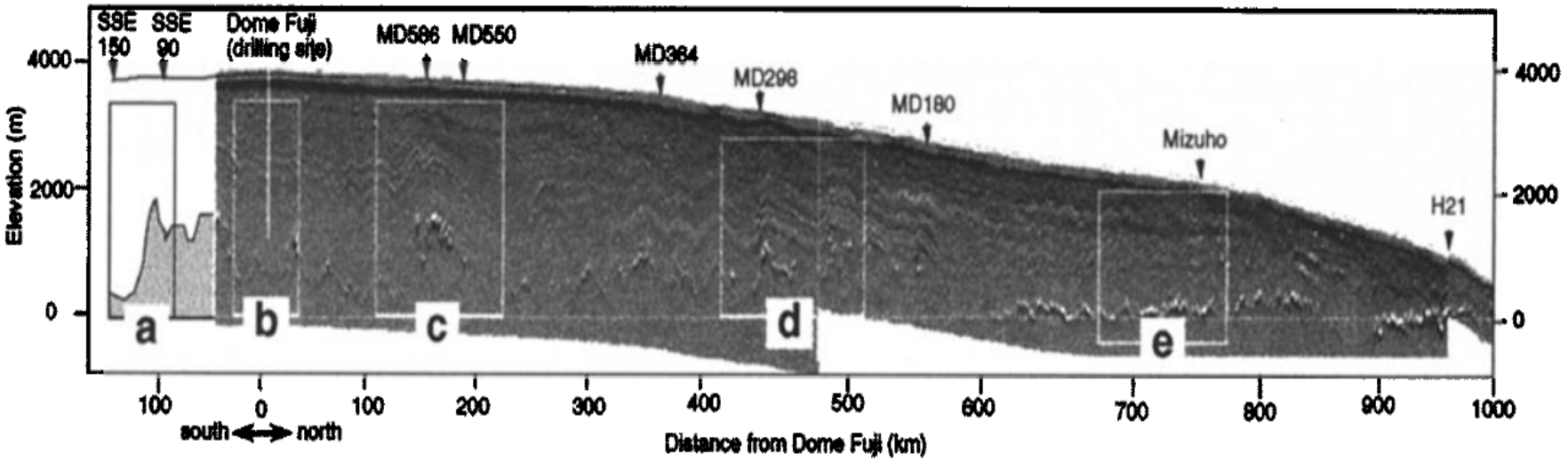

Figure 2. Cross section map of the ice sheet along the 1150 km traverse line. Z-scope images (radar returns versus both depth and distance along the traverse) are from *Maeno et al.* [1994, 1996]. The 10 sites of detailed local measurements and the five areas (a-e) of cross section analyses are indicated. Note that the image is the first derivative of the received power along depth based on the 179-MHz measurement using a 1000-ns pulse. The section southeast of SSE40 was not measured.

Deep ice cores in Antarctica and Greenland

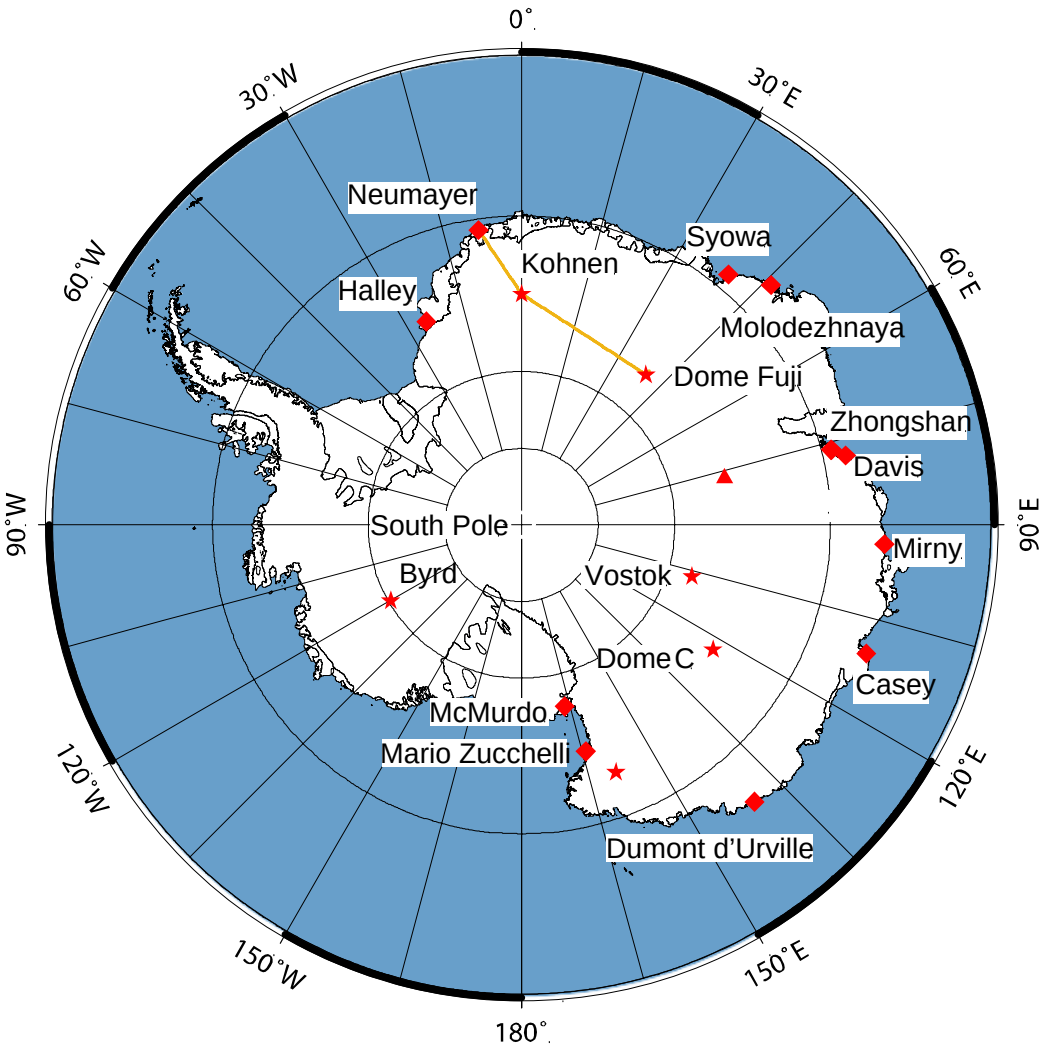

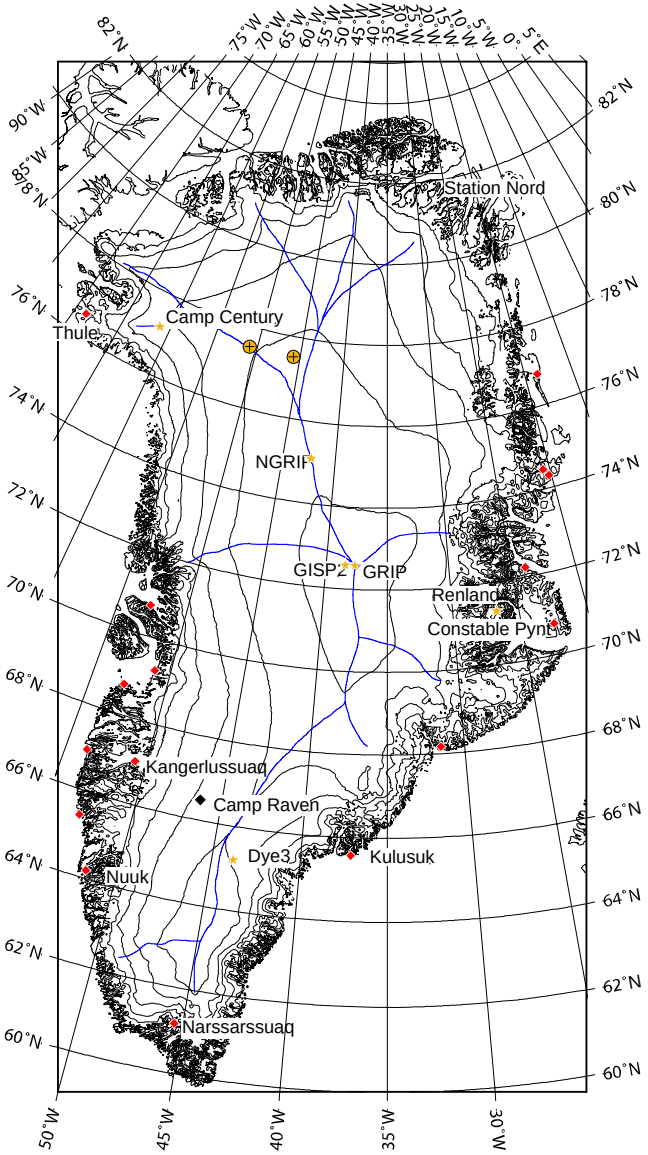

Antarctic Digital Database, Ekholm, 1998, maps by Steinhage with modifications

Internal horizons at ice core drill sites

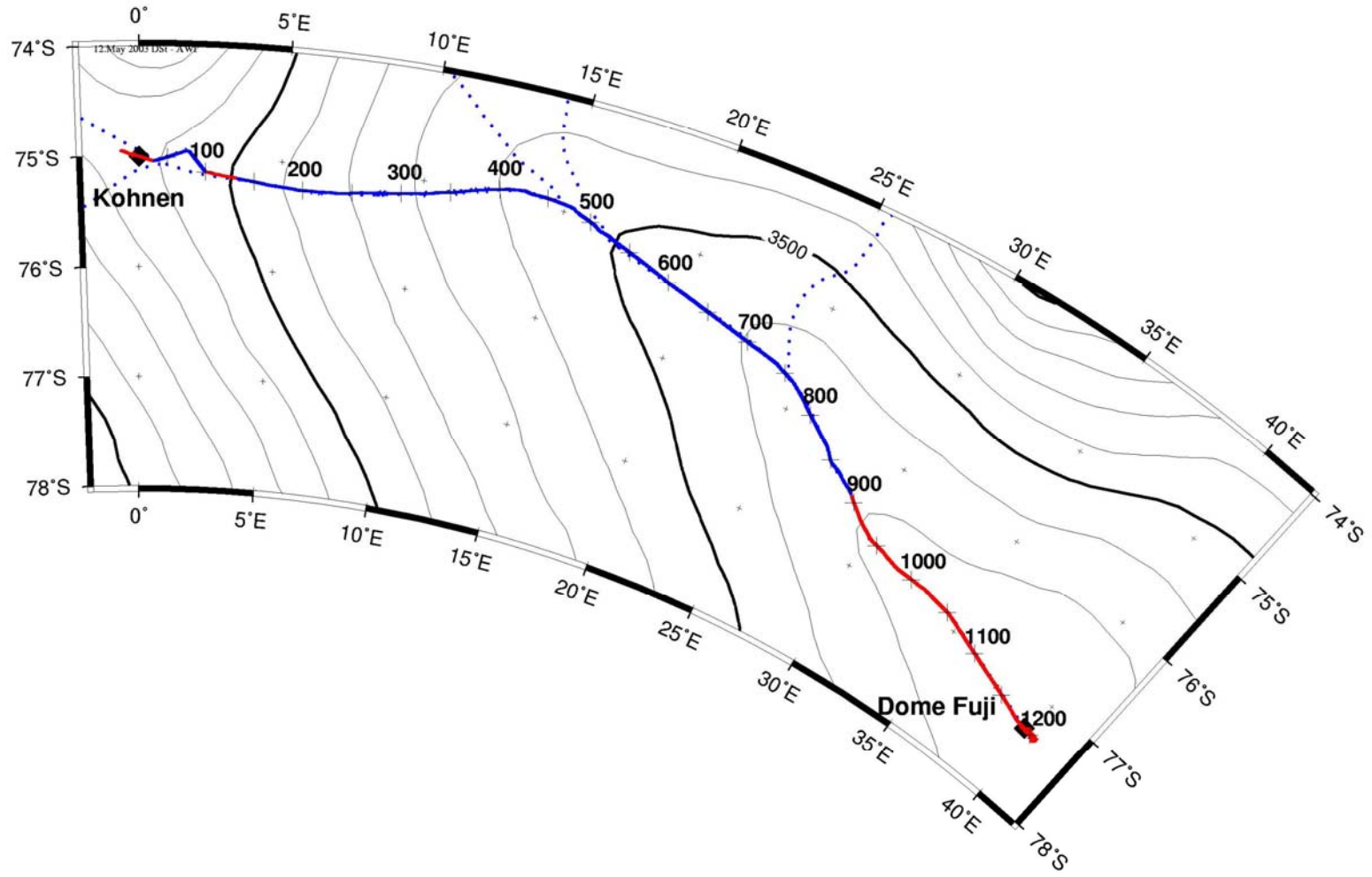

Internal horizons at ice core drill sites

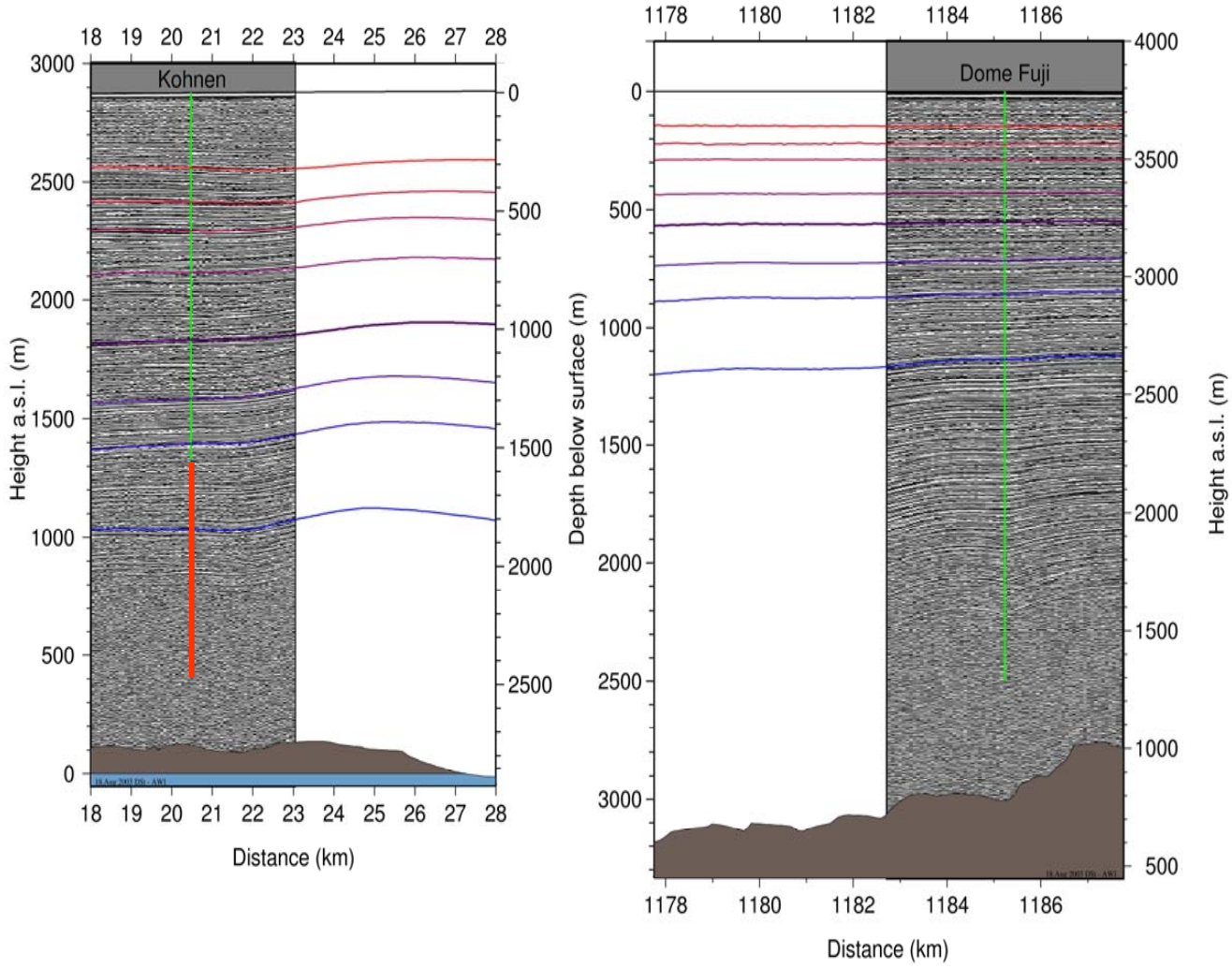

Internal horizons at ice core drill sites

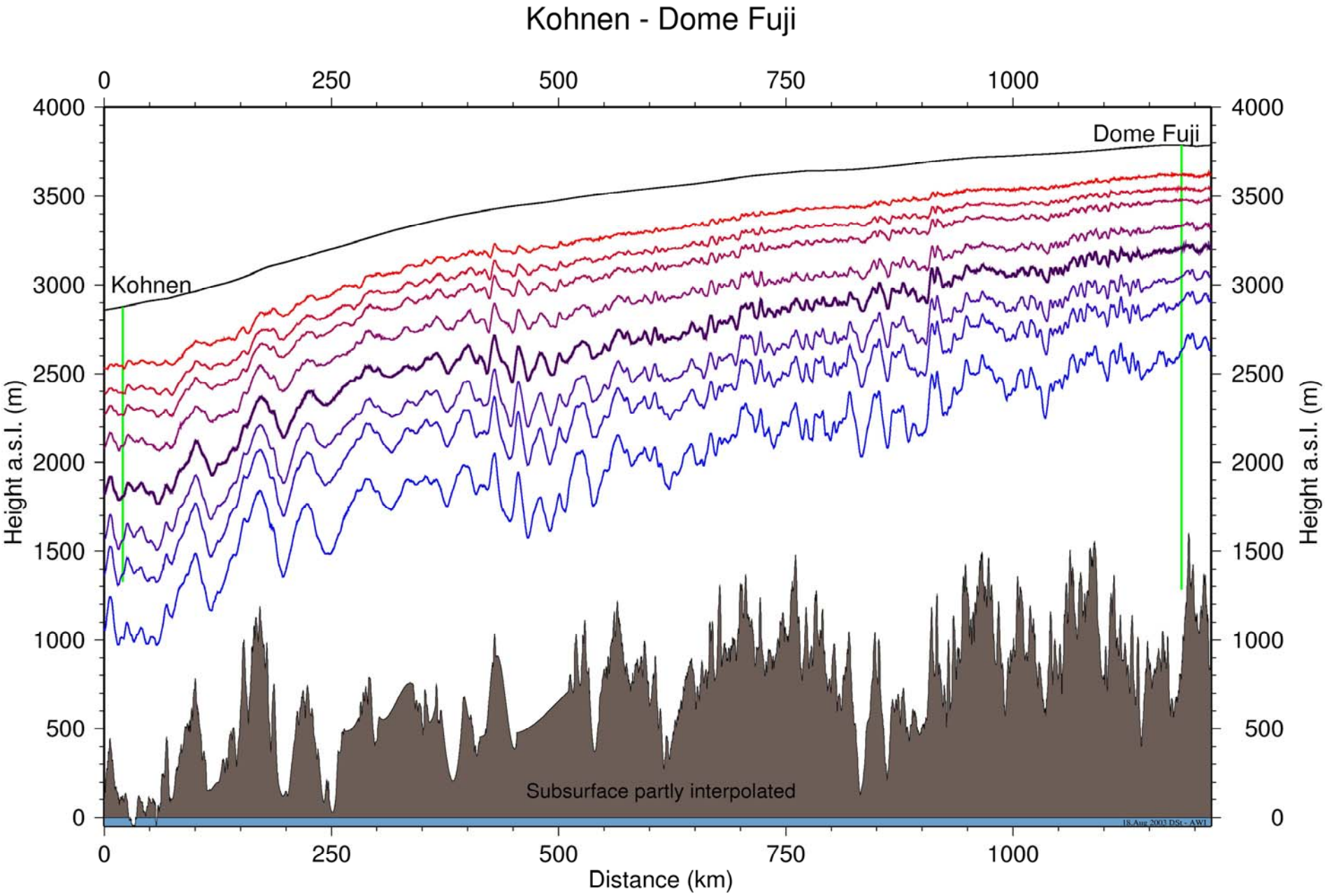

Linking Ice Cores and surveys in East Antarctica

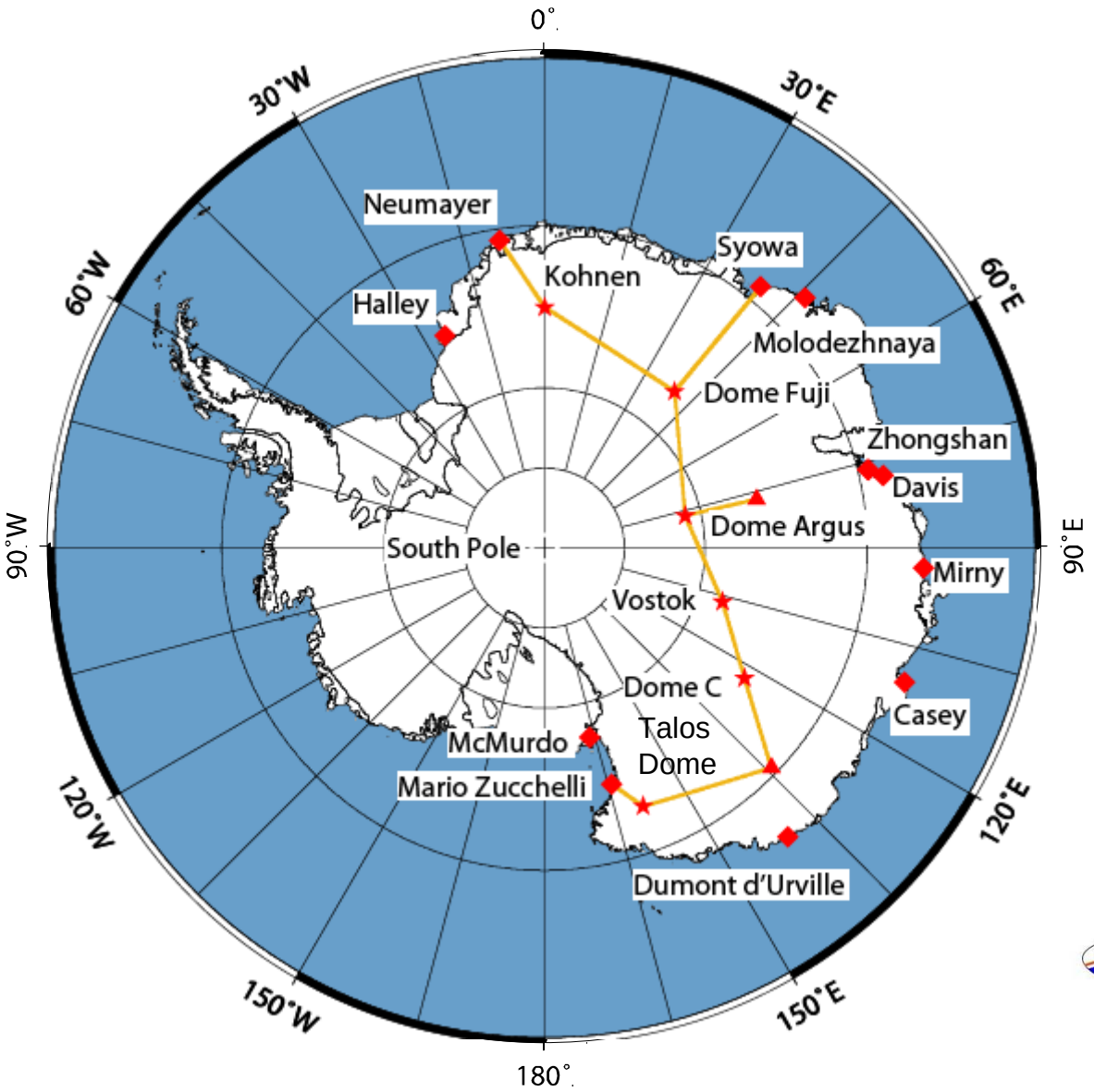

map: Daniel Steinhage
data: Antarctic Digital Database

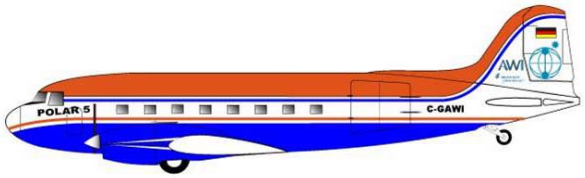

POLAR 5 (C-GAWI)

bi-refringence

(calcspar)

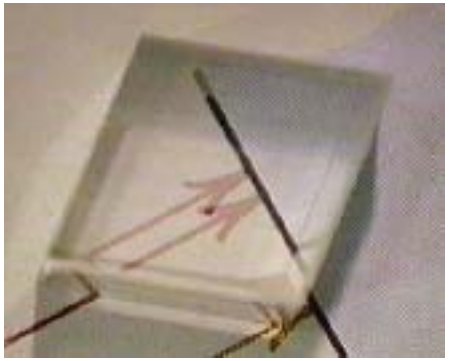

ordinary +
extra ordinary

with polarizer
ordinary

polarizer 90°
extra ordinary

http://hyperphysics.phy-astr.gsu.edu

Antarctic snow crystals

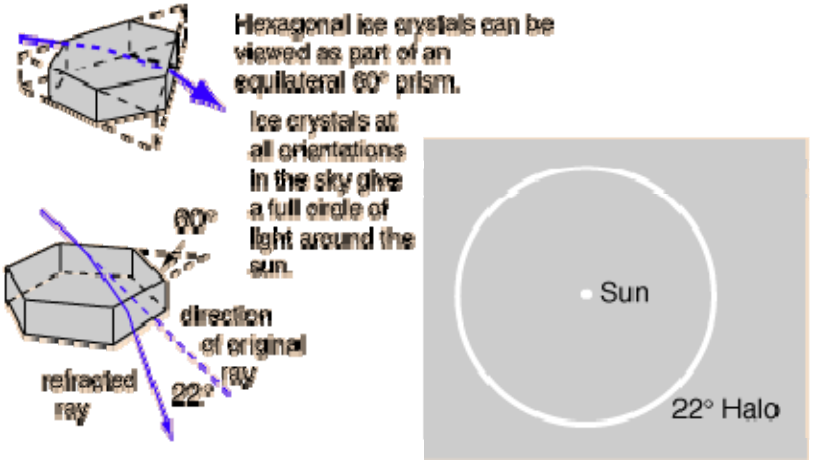

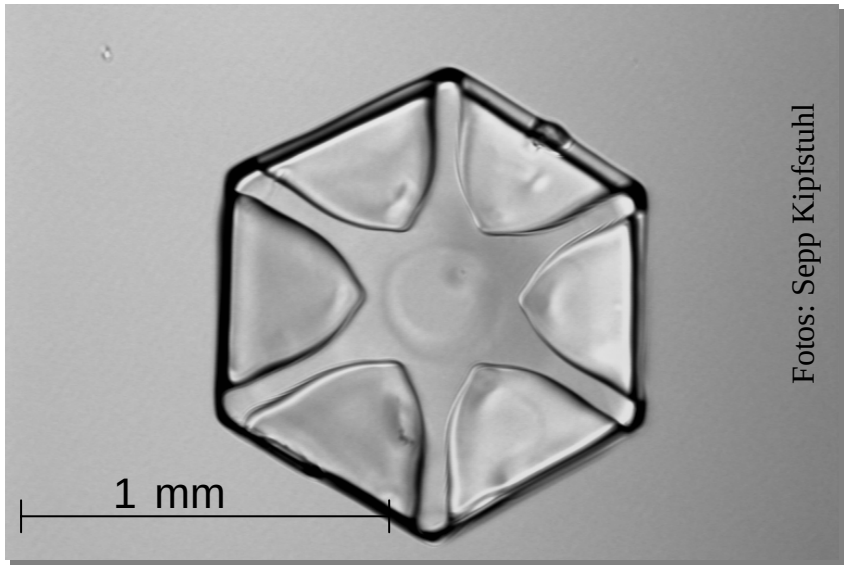

(Kohnen, Sommer 2003)

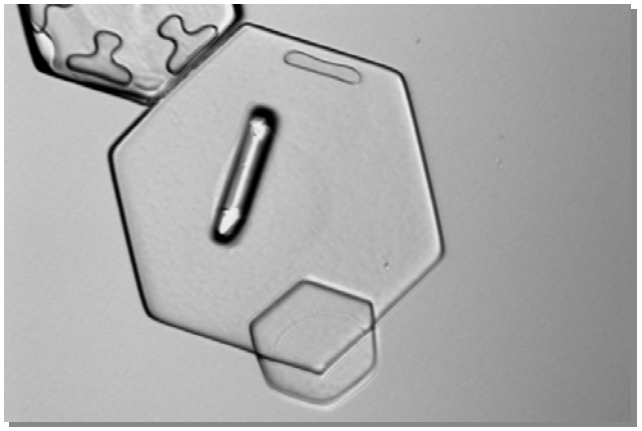

http://hyperphysics.phy-astr.gsu.edu

Birefringence of Ice

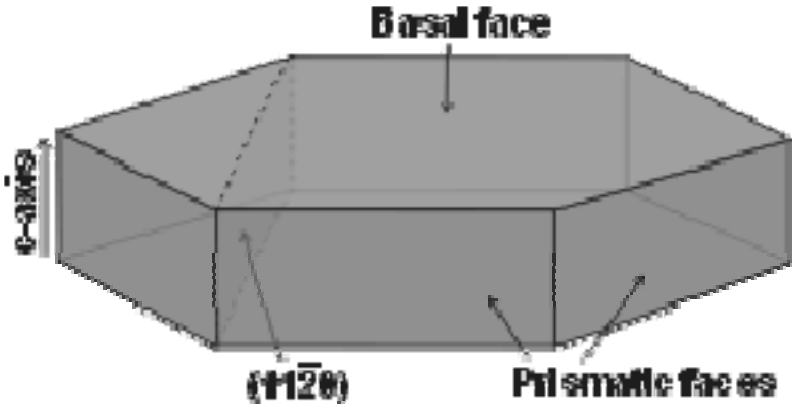

http://www.lsbu.ac.uk/water/ice1h.html

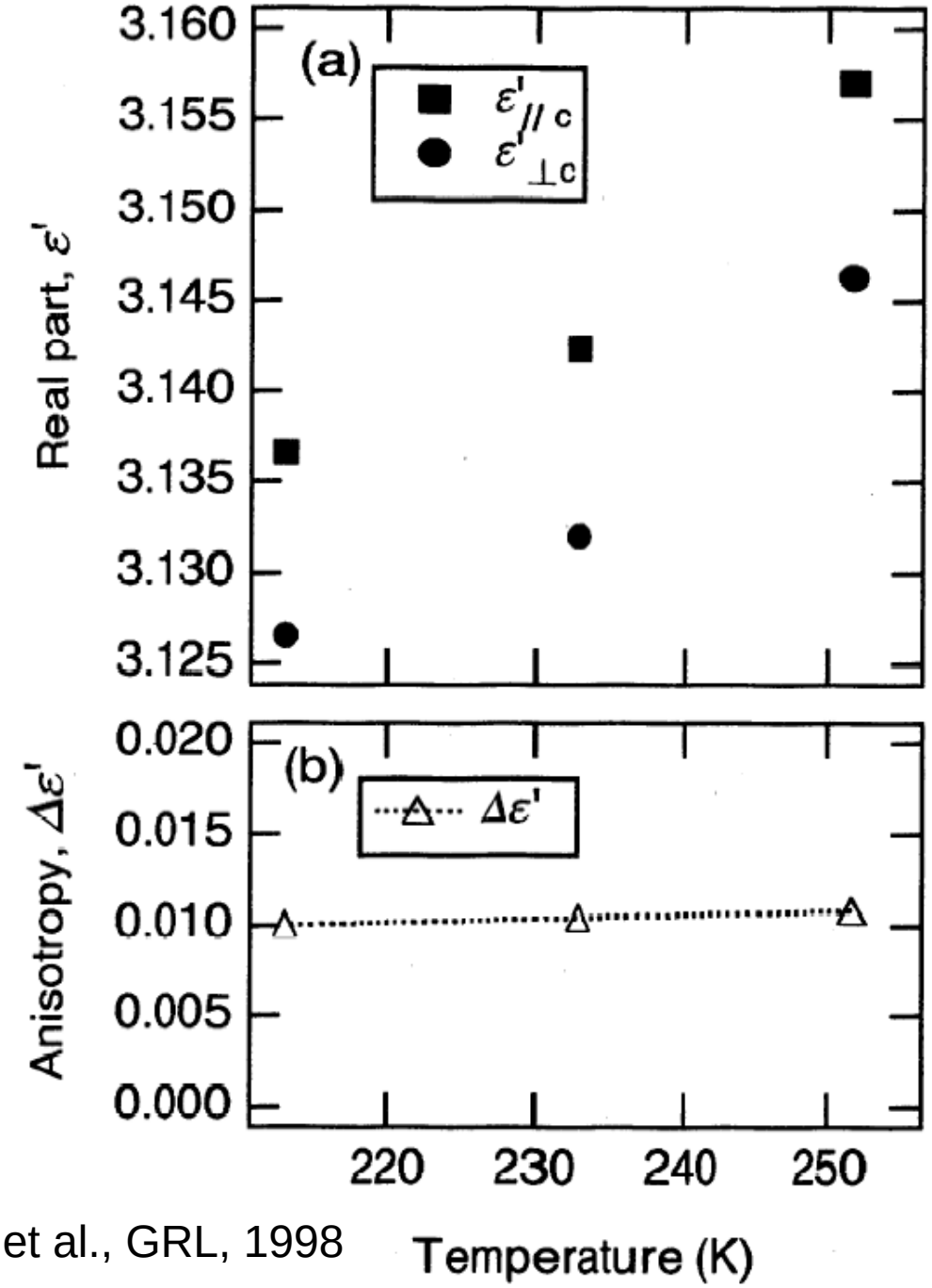

Matsuoka et al., GRL, 1998

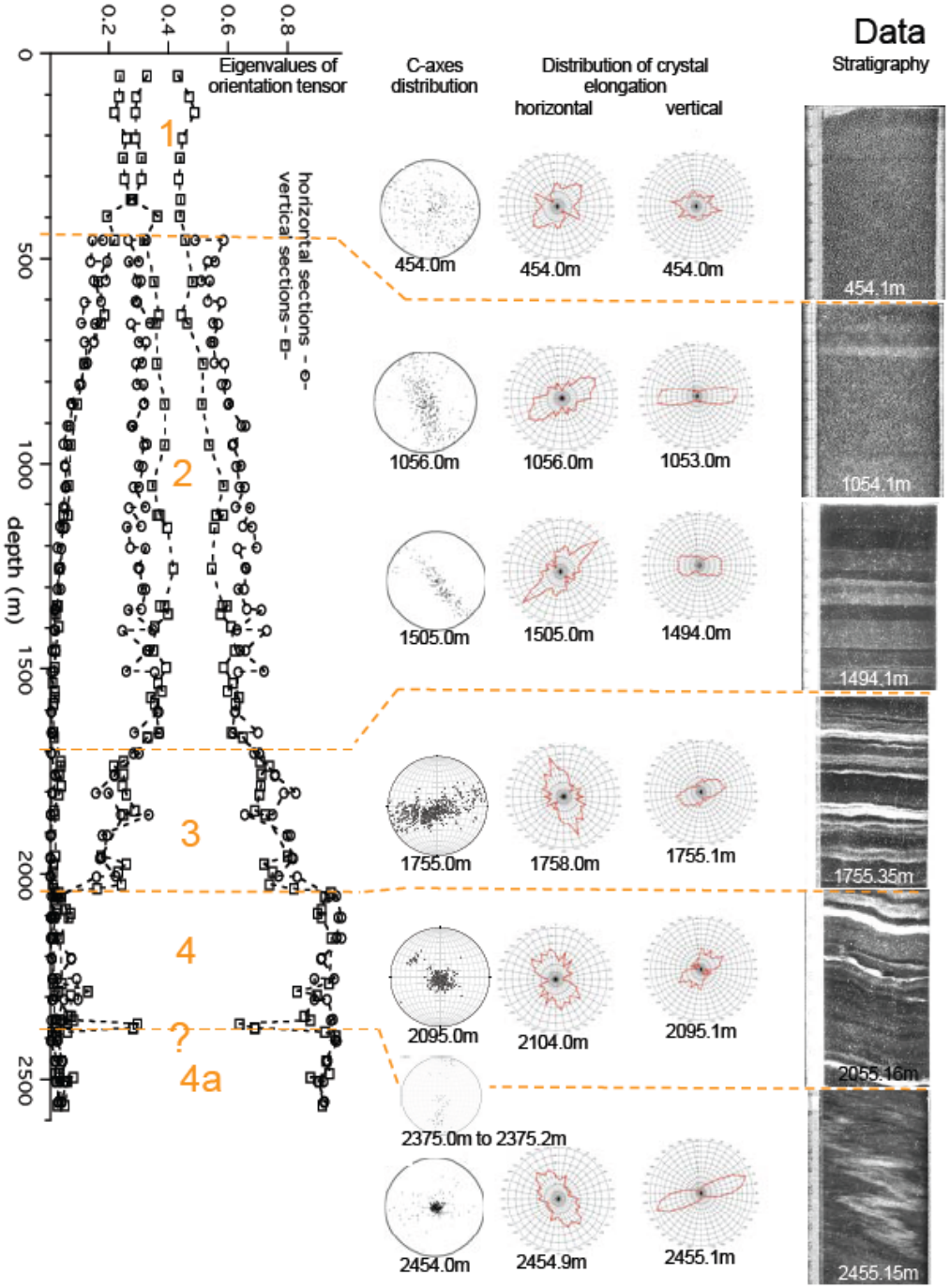

c-axis-orientation in the EDML ice core

Hamann et al., pers comm.

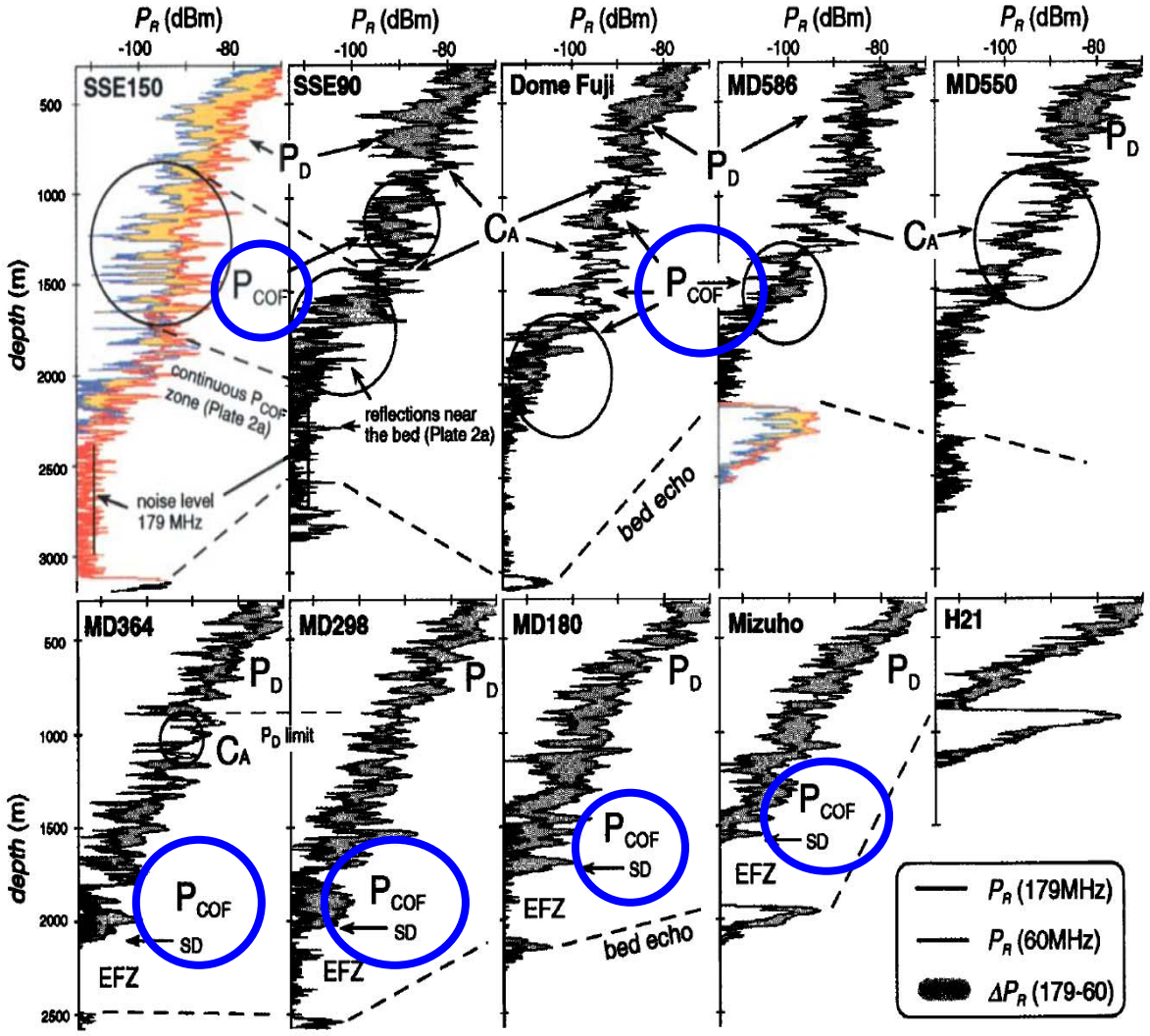

Plate 1. A-scope profiles at the 10 sites of detailed local measurements. Red and blue lines are $P_R(179)$ and $P_R(60)$, respectively. The variation of ΔP_R (equal to $P_R(179)$ - $P_R(60)$) with depth is shown in yellow. The dominant reflection mechanisms at various depth ranges are shown as P_D, P_{COF}, and C_A (see section 4). Detection limit (noise level) is at about -110 dBm. The profiles below this level are noise. Only when sudden drop of the signal is observed at transitions between significant signal and noise (indicated by "SD"), the depth range of the noise level is defined as the basal echo-free zone. It is indicated as EFZ.

FDTD synthetic radar traces

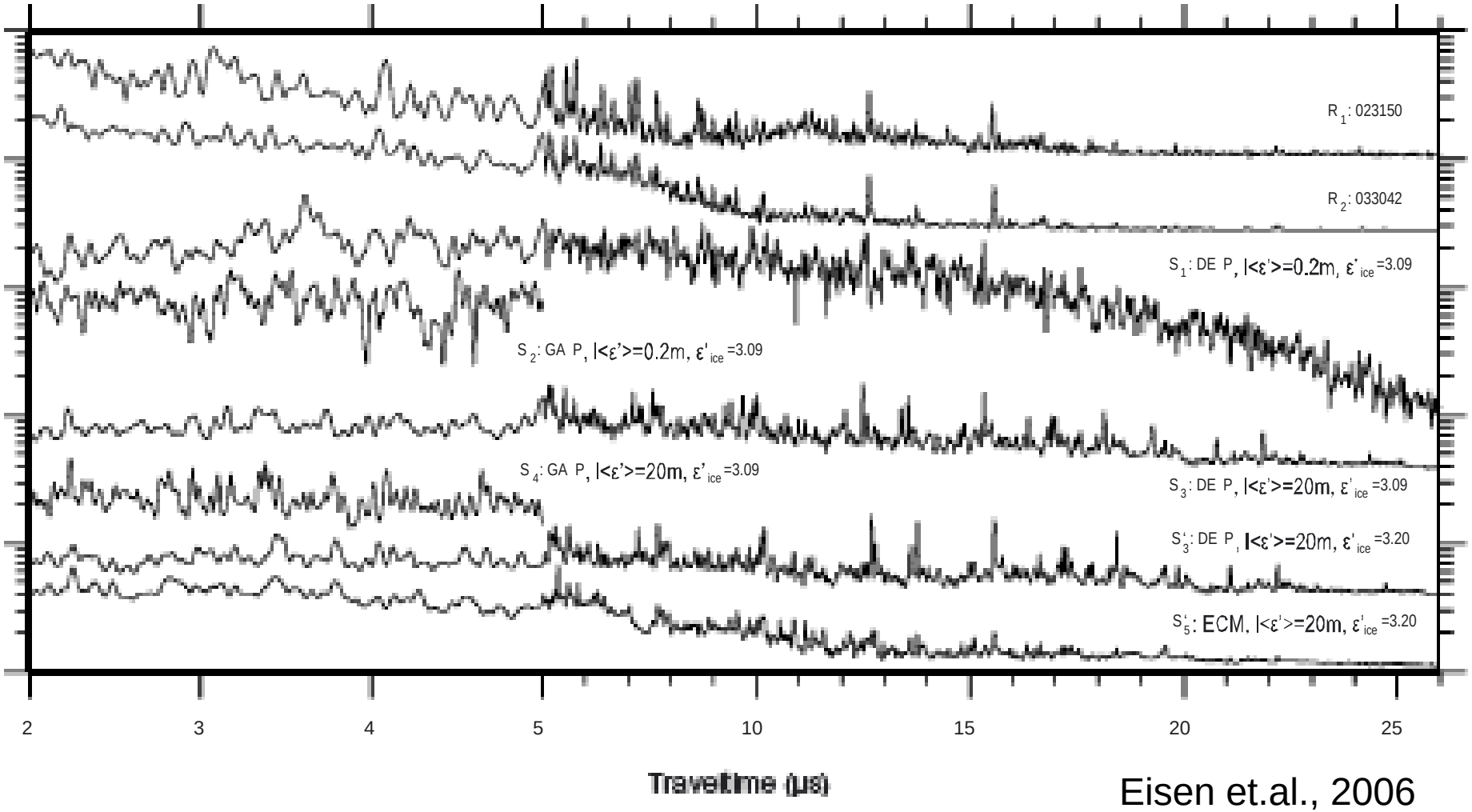

Eisen et.al., 2006

Genesis of radar reflectors

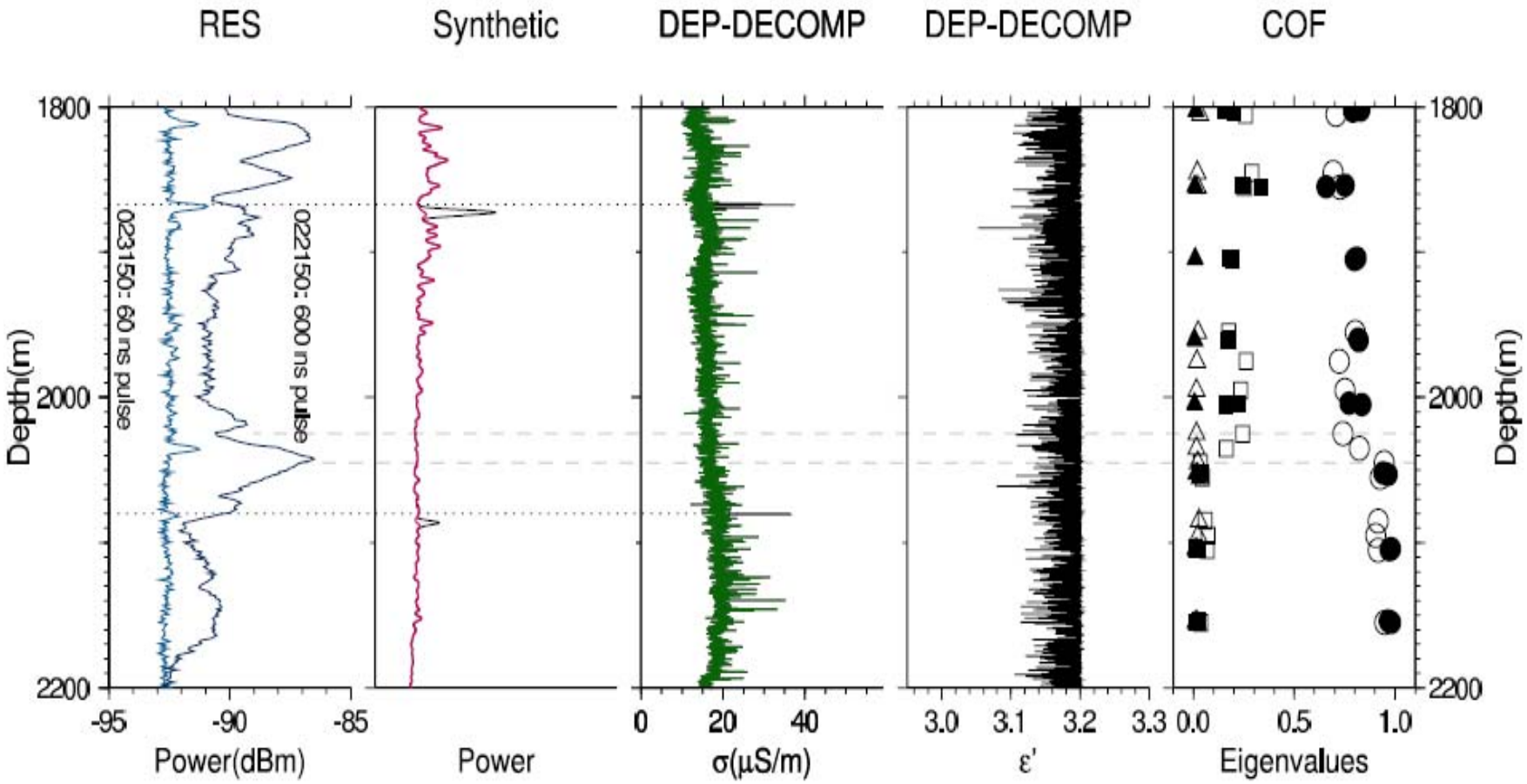

Fig. 3. Comparison of radar data and ice-core profiles at the EPICA-DML drill site. From left to right: RES signal power measured with two pulse widths for trace 4205 of profiles 022150 (600 ns pulse) and 023150 (60 ns pulse) with respect to 1 mW (dBm), representing a stack of 2000 recordings in total (200 pre-storage and 10 post-storage stacks) over a distance of 65 m; DEP-based synthetic RES trace for 60-ns pulse; DECOMP-corrected DEP conductivity (σ); DECOMP-corrected DEP-permittivity (ε', with the permittivity of pure ice as upper bound); eigenvalues (λ_1: triangle, λ_2: square, λ_3: circle) of crystal orientation tensor along horizontal (filled symbols) and vertical core samples (open symbols). The black synthetic trace is based on original conductivity data (black σ-curve); on top the red synthetic trace is plotted, based on the DEP data with conductivity peaks removed (green σ-curve); peaks originating from conductivity thus appear black, emphasized by dotted horizontal lines; dashed horizontal lines connect the depth of the strong RES reflector with transition depth of changes in COF.

Eisen et al.,
The Cryosphere, 2007

Crystal orientation fabrics (COF)

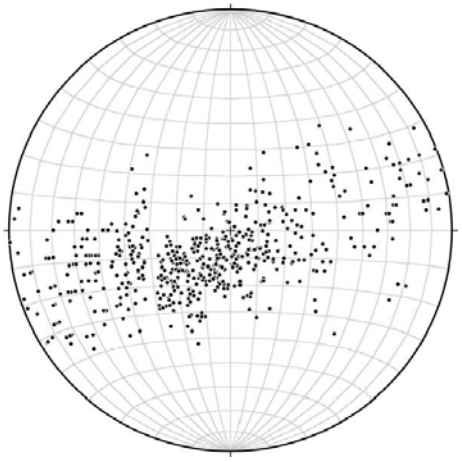

1755 m

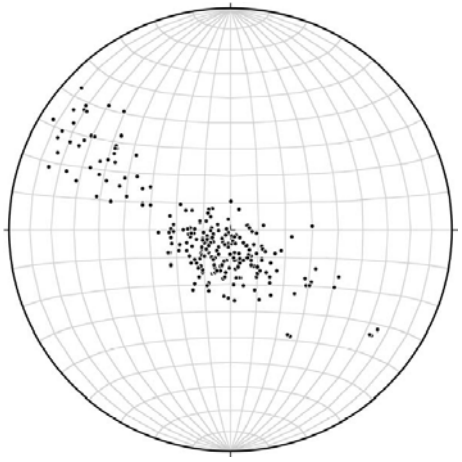

2036 m

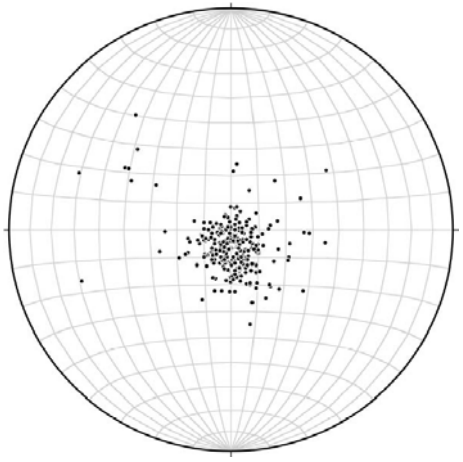

2046 m

Eisen et al., The Cryosphere, 2007

Modelling of ice sheets (local)

Journal of Glaciology, Vol. 54, No. 187, 2008

Application of a continuum-mechanical model for the flow of anisotropic polar ice to the EDML core, Antarctica

Hakime SEDDIK,[1] Ralf GREVE,[1] Luca PLACIDI,[2] Ilka HAMANN,[3]
Olivier GAGLIARDINI[4]

[1] *Institute of Low Temperature Science, Hokkaido University, Sapporo 060-0819, Japan*
E-mail: hakime@lowtem.hokudai.ac.jp
[2] *Department of Structural and Geotechnical Engineering, 'Sapienza', University of Rome, Via Eudossiana 18, I-00184 Rome, Italy*
[3] *Alfred Wegener Institute for Polar and Marine Research, Columbusstraße, D-27568 Bremerhaven, Germany*
[4] *Laboratoire de Glaciologie et Geophysique de l'Environment du CNRS (associéà l'Université Joseph Fourier–Grenoble I), 54 rue Molière, BP 96, F-38402 Saint-Martin d'Hères Cedex, France*

ABSTRACT. We present an application of the newly developed CAFFE model (Continuum-mechanical, Anisotropic Flow model based on an anisotropic Flow Enhancement factor) to the EPICA ice core at Kohnen Station, Dronning Maud Land, Antarctica (referred to as the EDML core). A one-dimensional flow model for the site is devised, which includes the anisotropic flow law and the fabric evolution equation of the CAFFE model. Three different solution methods are employed: (1) computing the ice flow based on the flow law of the CAFFE model and the measured fabrics; (2) solving the CAFFE fabric evolution equation under the simplifying assumption of transverse isotropy; and (3) solving the unrestricted CAFFE fabric evolution equation. Method (1) demonstrates clearly the importance of the anisotropic fabric in the ice column for the flow velocity. The anisotropic enhancement factor produced with method (2) agrees reasonably well with that of method (1), even though the measured fabric shows a girdle structure (which breaks the transverse isotropy) in large parts of the ice core. For method (3), we find that the measured fabric is reproduced well by the model down to ∼2100 m depth. Systematic deviations at greater depths are attributed to the disregard of migration recrystallization in the model.

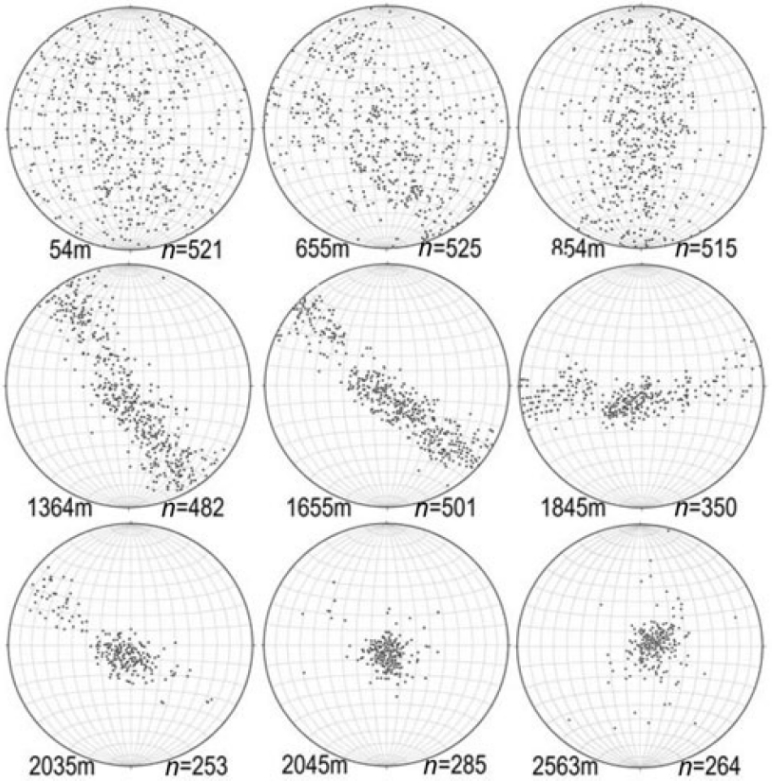

Fig. 5. Selected Schmidt diagrams for the observed fabrics of the EDML ice core between depths of 54 and 2563 m. Centres of diagrams coincide with the core axis. All examples displayed here are from vertically cut thin sections, rotated to the horizontal view. *n* denotes the number of grains included. Note that the orientations of the horizontal planes with respect to the ice-flow direction are unknown.

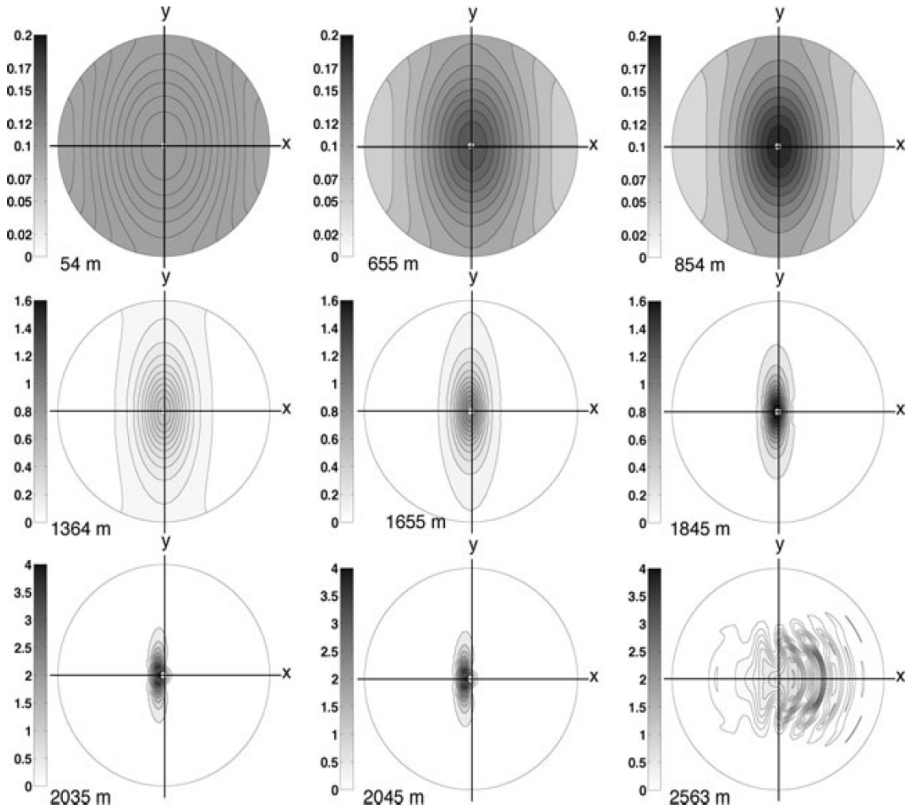

Fig. 11. Schmidt diagram representation of the EDML fabrics (ODF) at depths between 54 and 2563 m computed by Equation (32). As in Figure 5, the centres of the diagrams coincide with the core axis and the projection is on the horizontal (x–y) plane.

X-ray Laue diffraction

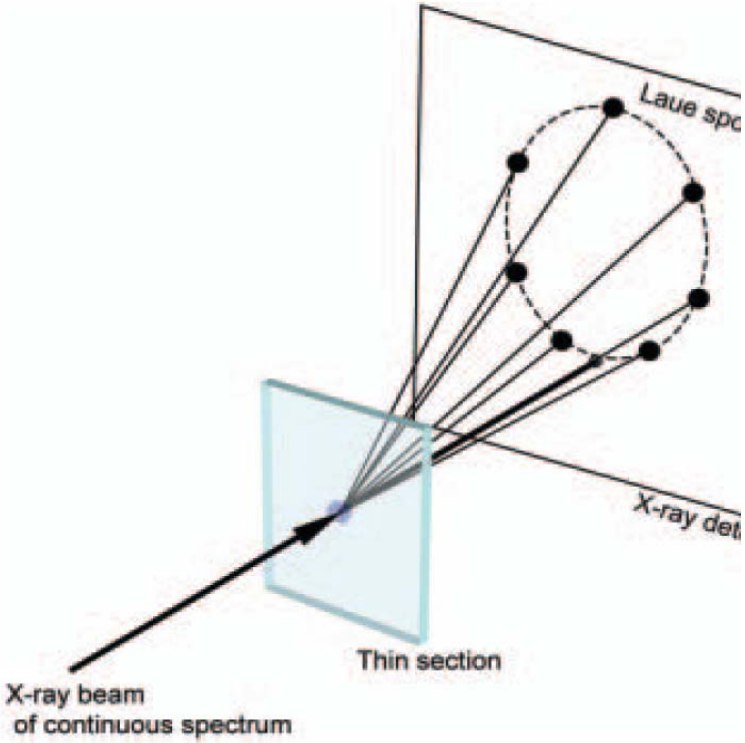

Fig. 1. The experimental arrangement for a transmissi method.

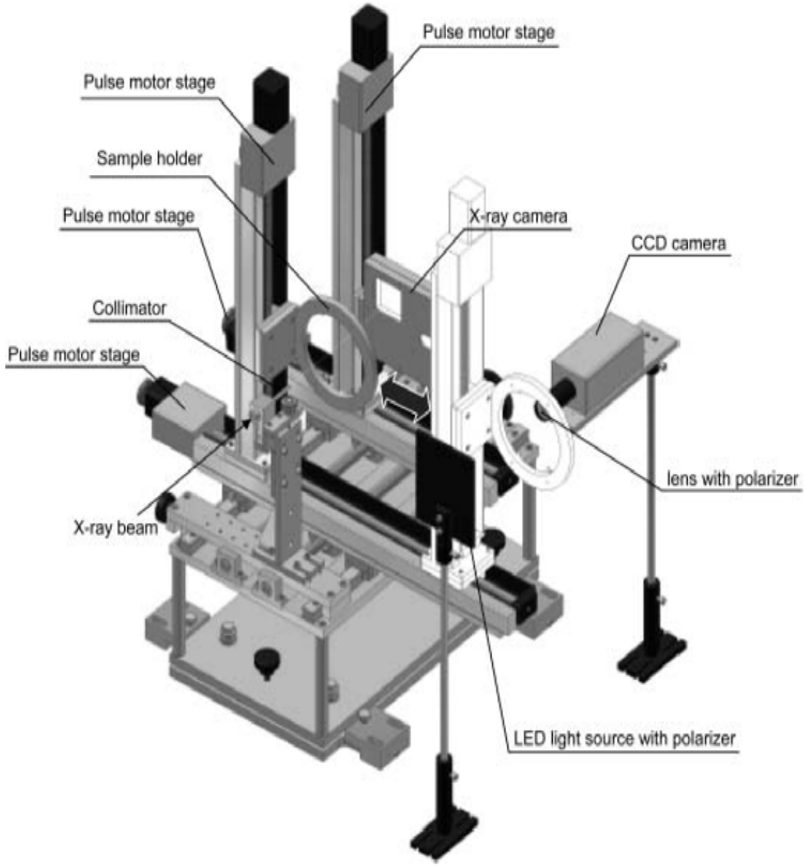

Fig. 2. The X-ray device.

Miyamoto et al., Ann. Glaciol., 42, 2005

X-ray Laue diffraction and microstructure mapping

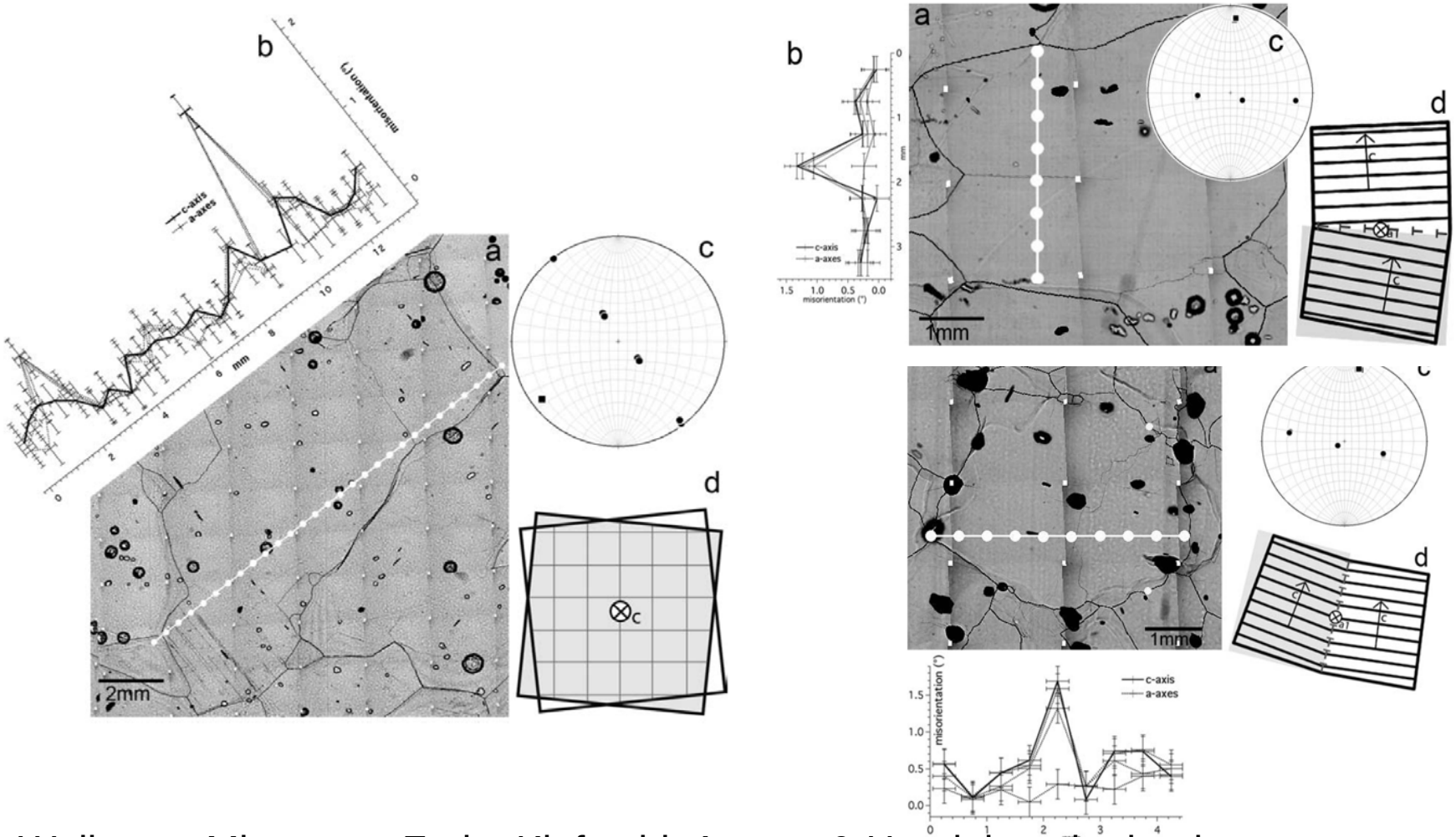

Weikusat, Miyamoto, Faria, Kipfstuhl, Azuma & Hondoh, submitted

Precise measurement of dielectric anisotropy in ice Ih at 39 GHz

Takeshi Matsuoka,[a] Shuji Fujita, Shigenori Morishima,[b] and Shinji Mae
Department of Applied Physics, Faculty of Engineering, Hokkaido University, N13 W8, Sapporo 060, Japan

(Received 23 October 1996; accepted for publication 25 November 1996)

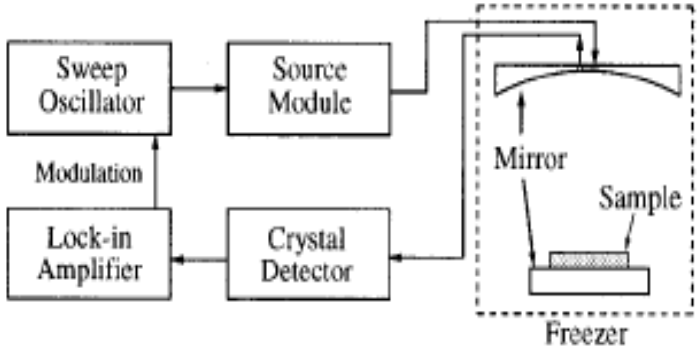

FIG. 1. The vertical arrangement of the open resonator and the experimental setup.

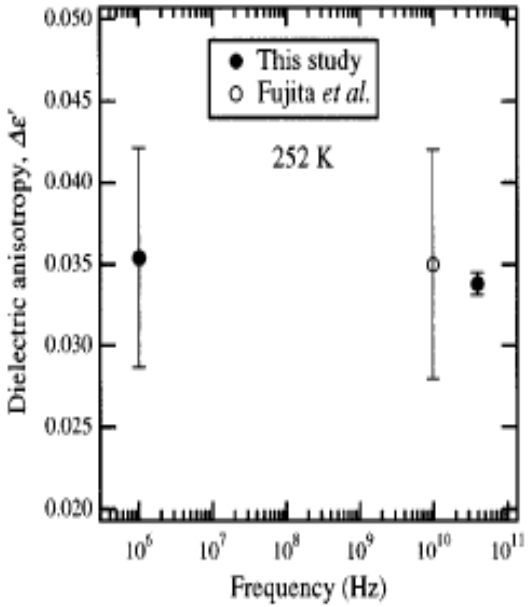

FIG. 6. Frequency dependence of the dielectric anisotropy, $\Delta\epsilon'$. The solid symbols represent the measured values in this study, and the open symbols represent the results of Fujita and co-workers (Ref. 15).

JOURNAL OF GEOPHYSICAL RESEARCH, VOL. 114, F03023, doi:10.1029/2008JF001143, 2009

Metamorphism of stratified firn at Dome Fuji, Antarctica: A mechanism for local insolation modulation of gas transport conditions during bubble close off

Shuji Fujita,[1] Junichi Okuyama,[2,3] Akira Hori,[2,4] and Takeo Hondoh[2]

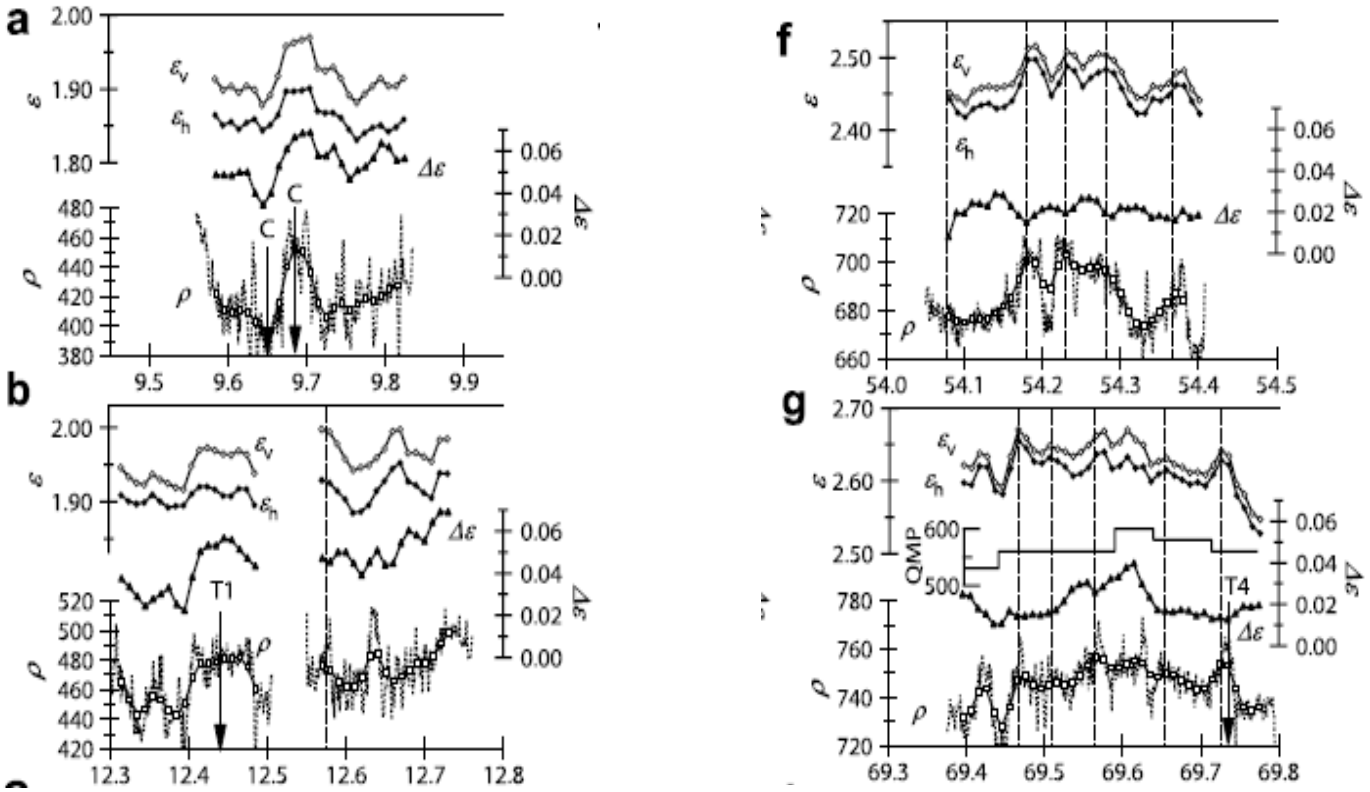

X-ray tomography

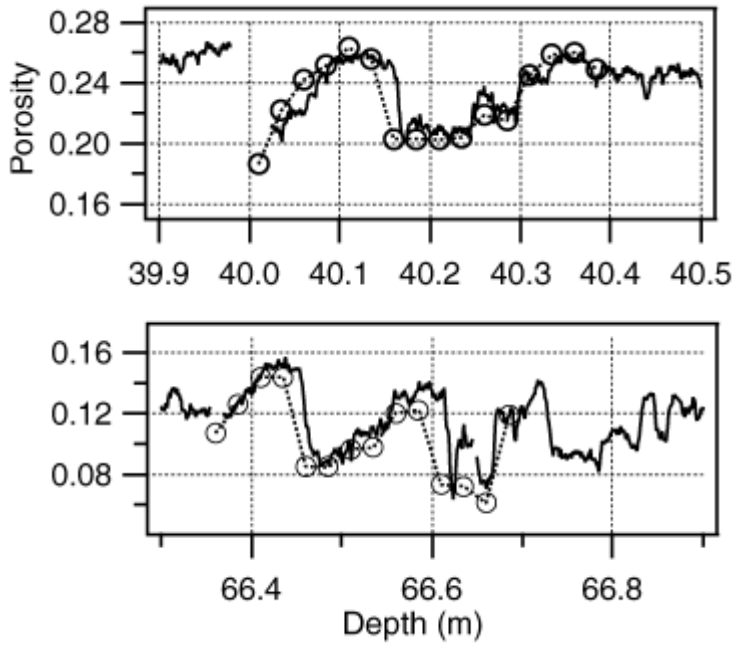

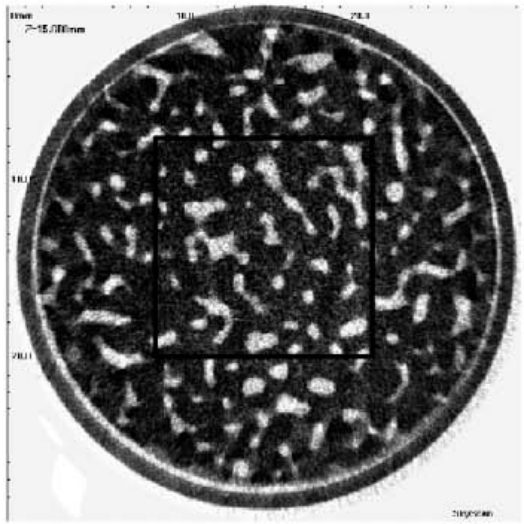

a

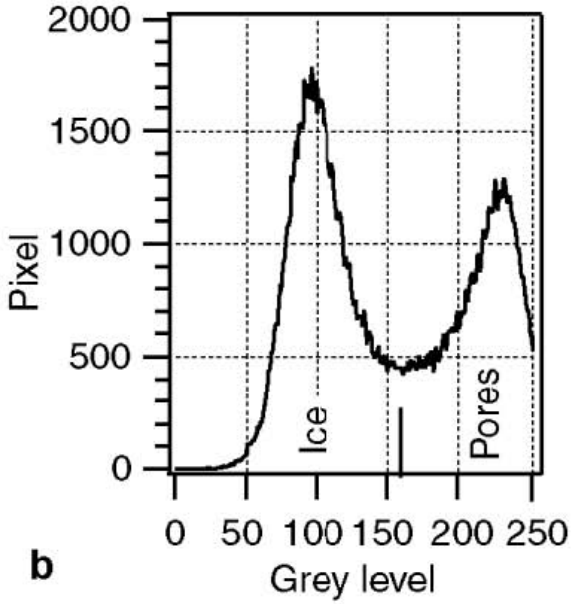

b

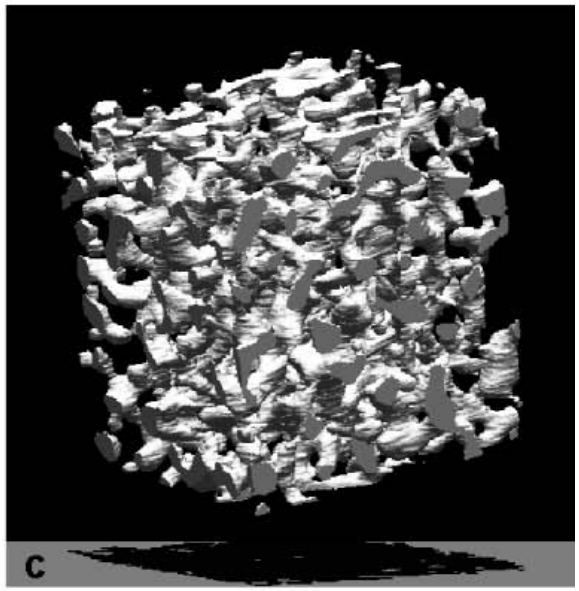

c

Freitag, Wilhelms, Kipfstuhl, JGlaciol, 2004

Orbital Tuning of ice cores

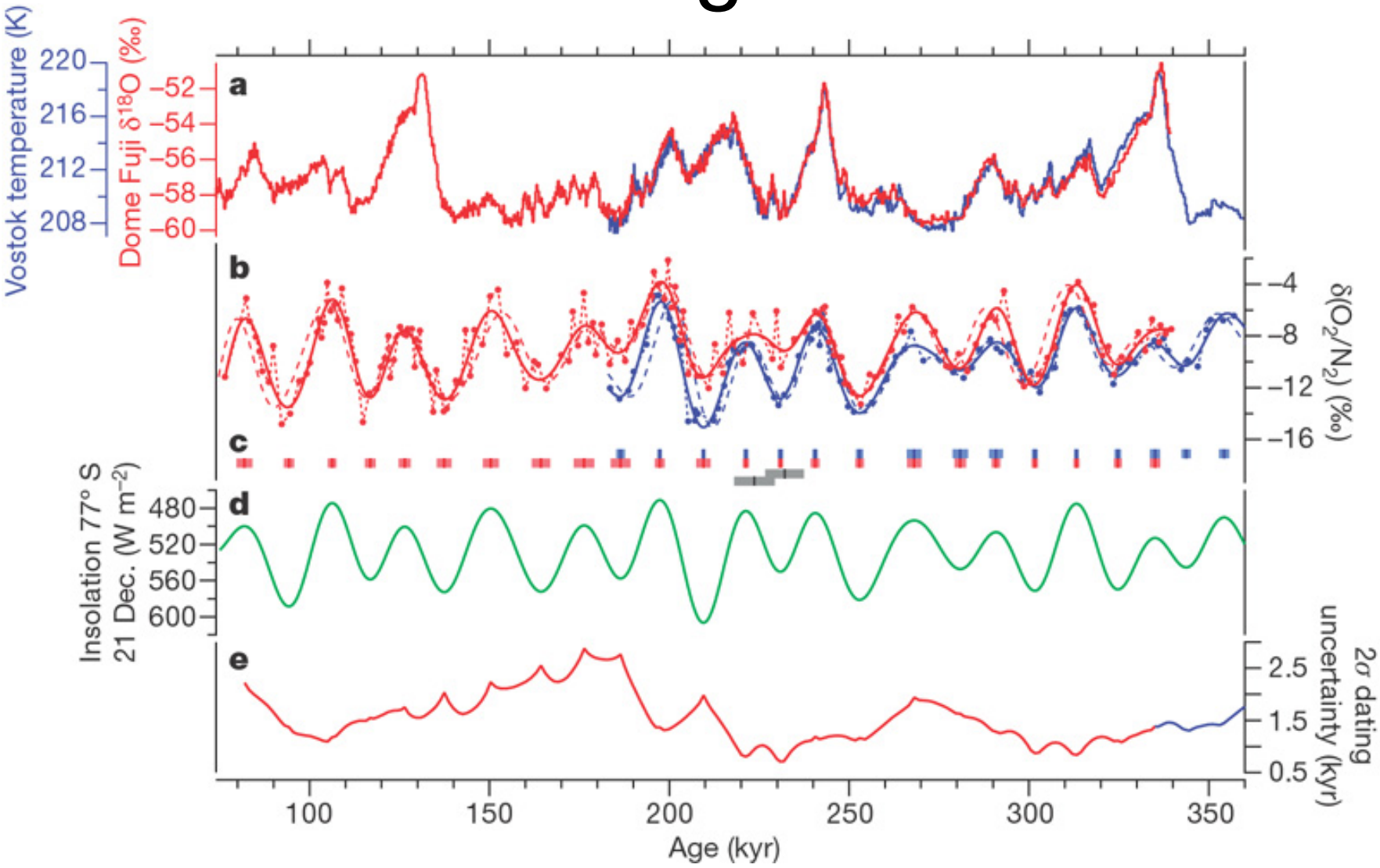

Kawamura et al., 2007

Summary (Frontiers in Low Temperature Science) – my own opinion

Understand the micro-physical properties of ice and its pore-space

apply them to a better understanding of the behaviour of ice sheets under different environmental conditions

apply them to a better founded reconstruction of proxies of past environmental conditions